Whole-Cell Patch Clamp Investigations on Rapid Synaptic Scaling of Mouse CA1 Pyramidal Neurons under Optogenetic Stimulation

Master's Thesis in Applied Biochemistry, KBKM05

Author:	Leonard Groth	leonard.groth.843@student.lu.se
Examiner:	Prof. Leif Bülow	leif.bulow@kilu.lu.se
Principal supervisor:	Prof. Mérab Kokaia	merab.kokaia@med.lu.se
Assistant supervisor:	Marco Ledri, PhD	marco.ledri@med.lu.se
Opponent:	My Andersson, PhD	my.andersson@med.lu.se
Date:	2021-01-28	

The best-laid plans of mice and men often go awry

A B S T R A C T

The brain consists of billions of neurons forming intricate contiguous networks. The connective strength in these networks change throughout life in response to experience and environmental stimuli. Indeed, by using these plastic mechanisms *You* have successfully molded networks in your brain to perform the task of reading and understanding this text. This feat is made more remarkable when considering that learning these things did not come at the expense of network stability. However, not all experiences are the same and some, such as flashing lights, can in fact cause sickness.

Healthy brains are achieved and maintained by homeostatic plasticity, a set of physiological mechanisms that stabilize network activity. Synaptic scaling is one such mechanism that up- or down-regulates the firing-rates of individual neurons by changing the number of postsynaptic glutamate receptors in a cell-autonomous fashion. Synaptic scaling is thought to occur over hours, yet in order for homeostatic plasticity to work it must match the speed at which destabilizing forms of plasticity accumulate. The speed at which this happens is currently unknown for any cell, and it is therefore interesting to see if synaptic scaling happens more quickly in response to pathologies of network instability such as epilepsy.

To investigate this, we measured changes in mean amplitude and interevent intervals of spontaneous excitatory postsynaptic currents in CA1 pyramidal neurons from acute hippocampal slices of CAMKIICre-ChR2 mice. This was done before, during and after optogenetic stimulation intended to model epileptic seizures using whole-cell patch clamping.

The gathered results suggest that no presynaptic modulation occurs in response to the stimulation but were inconclusive on changes to postsynaptic function. Going forward, a different experimental setup is required in order to rule out the existence of rapid synaptic scaling as a natural anticonvulsive mechanism in epilepsy.

TABLE OF CONTENTS

1. Introduction 5
1.1 Aim 5
2. Background 6
2.1 Fundamental neuroscience 6
2.1.1 Electrochemical dynamics of neurons 7
2.1.1.1 Resting potential: the baseline 9
2.1.1.2 Action potential: the voltage-gated outgoing signal 9
2.1.1.3 Synaptic transmission 10
2.1.1.4 AMPARs in the central nervous system 11
2.1.1.5 Graded potential: the ligand-gated incoming signal 12
2.2 Electrophysiology 14
2.2.1 The patch clamp technique 14
2.2.1.1 Patch clamp configurations 16
2.2.1.2 Electrical equivalent circuit model of patch clamping 17
2.3 Optogenetics 19
2.3.1 Channelrhodopsins 19
2.3.2 Implementation of optogenetic system and Lox-Cre recombination 19
2.4 The hippocampal formation 20
2.4.1 Function of hippocampus 21
2.5 Neuroplasticity 21
2.5.1 Hebbian plasticity 21
2.5.1.1 Synaptic competition 22
2.5.1.2 Network stability problems 22
2.5.2 Homeostatic plasticity 23
2.5.2.1 Synaptic scaling 24
2.6 Epilepsy 25
3. Methods 27
3.1 Animals 27
3.2 Acute hippocampal slice preparation 27
3.3 Whole-cell patch clamp recordings 27
3.4 Optogenetic stimulation 28
3.5 Data analysis 28

4. Results 30
4.1 Changes to sEPSC interevent intervals 33
5. Discussion 35
5.1 Experimental design 35
5.1.1 Consequences of placing ChR2 under the CaMKII promotor 35
5.1.2 Consequences of voltage clamping 36
5.1.2.1 VC prevents AP generation differently from TTX 36
5.1.3 Space clamping issues 37
5.1.4 Consequences of whole-cell patch clamping 37
5.1.5 Importance of electrochemical dynamics 38
5.1.6 Summary of potential design flaws 38
5.2 Future experimental design 39
Populärvetenskaplig sammanfattning 41
Acknowledgements 42
References 43

1. Introduction

Epilepsy is a family of diseases of the brain that are characterized by a propensity to generate epileptic seizures; ictal brain states with abnormally synchronized neuronal activity. Approximately 1% of the global population has epilepsy [2], and the socioeconomic burden of this is well reflected in epilepsy's estimated annual cost of 15.5 billion dollars in the US alone [3]. Despite this, there is still no universal treatment or cure for epilepsy, and current antiepileptic drugs have extensive side-effects that leave much to be desired [2]. This dissatisfying status quo underscores the urgent need for continued epilepsy research.

Today, much epilepsy research focuses on how seizures start. This fails to capture an essential component of epilepsy, namely that seizures eventually end. Seizures are not particularly long, spanning minutes at most before self-terminating [4]. Seizure termination, although poorly understood, is fundamentally a return to an operationally healthy brain state (or rather, an interictal state) [5]. Healthy brain states are achieved and maintained by homeostatic plasticity, a set of physiological mechanisms that equipoise cellular intrinsic excitability to synaptic strength as well as network excitation to network inhibition. Through homeostatic plasticity, neurons are able to finetune their own excitability relative to overall network activity [6].

Synaptic scaling is a homeostatic plasticity mechanism that regulates network activity through negative feedback. It is thought to work by scaling the number of α-amino-3-hydroxy-5-methyl-4-isoxazolepropionic acid receptors (AMPARs) on postsynaptic terminals up (or down) in response to low (or high) activity [7]. Considering that AMPARs are also key mediators in epileptic seizures [8] it seems possible that synaptic scaling is somehow involved in seizure self-termination.

Despite this, there is to our knowledge no research on the scaling of AMPARs during and after a seizure. Perhaps this is because synaptic scaling is generally thought to take place over hours to days [7, 9] – much larger timescales than epileptic seizures span.

1.1 Aim

Opposing the popular belief that synaptic scaling is a slow phenomenon, we hypothesize that fast synaptic downscaling of AMPARs occurs through internalization in response to epileptic seizures in order for the brain to decrease overall neuronal excitability.

To investigate rapid synaptic downscaling, we measured changes in spontaneous excitatory postsynaptic currents (sEPSC) averages using whole-cell patch clamp on CA1 pyramidal neurons from acute hippocampal slices of CAMKIICre-ChR2 mice; before, during and after optogenetic stimulation intended to model epileptic seizures.

2. Background

Since this work concerns neuroscience it is essential for the reader to have a basic understanding on how the brain works. After an introduction to fundamental neuroscience, two techniques important to this work are reviewed – namely, patch clamping and optogenetics. Following this are brief reviews on neuroplasticity and epilepsy. This background is important to understand our choice of methods, our interpretation of the results and the basis of our discussion.

2.1 Fundamental neuroscience

The human brain is composed of approximately 10^{11} neurons of more than 1000 different cell-types, each of which typically connects to over 10^4 other neurons [1]. Neurons create intricate contiguous networks, and it is from their organization into anatomical circuits that the brain can marvel. The structure of neurons offers important insight into this organization.

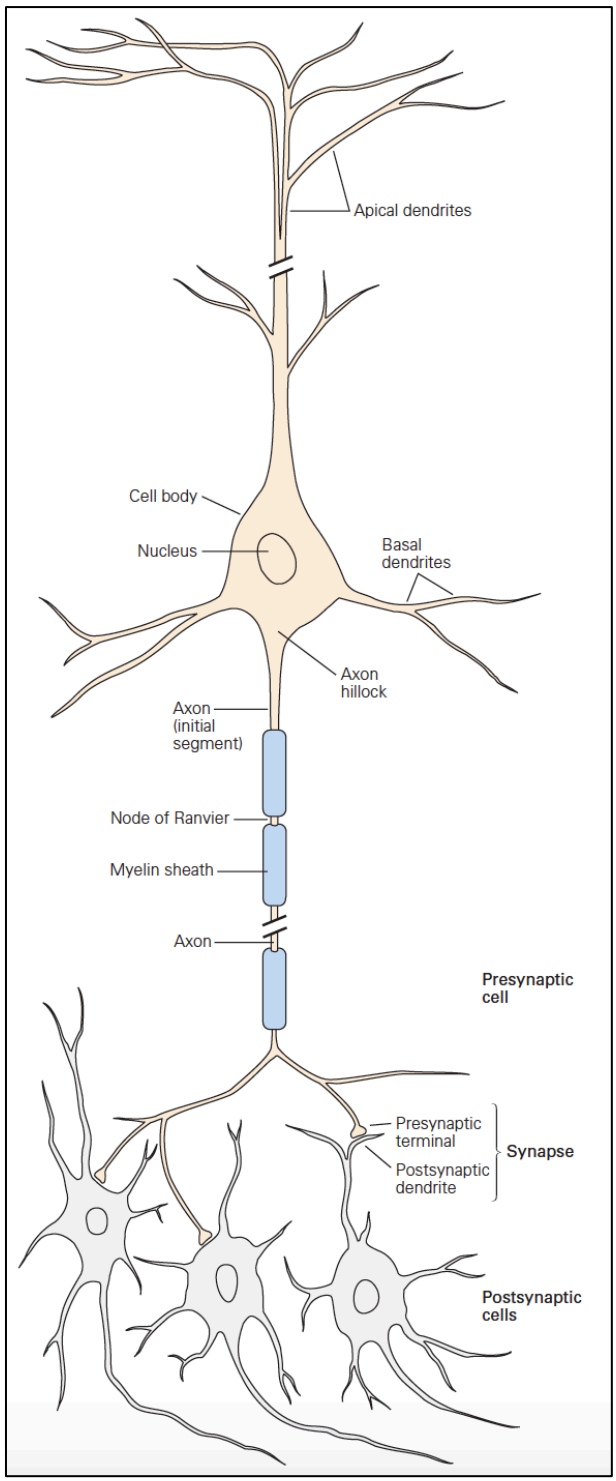

Figure 1 Structure of a typical neuron with cell body (soma), dendrites, axon and presynaptic terminals. Other parts typical for neurons are included too, such as nodes of Ranvier, myelin sheats and other sub-structures. Both axodendritic and axosomatic synapses are formed with postsynaptic cells in this figure [1].

Typical neurons have, roughly speaking, four functionally distinct areas called (i) dendrites, (ii) soma (iii) axon and (iv) presynaptic terminals (see Figure 1) [1]. Neurons that project outside their anatomical structure are called principal neurons, whereas those that project within their structure are called interneurons [10]. Generally, dendrites mediate signal input from other neurons, which is then transmitted to the soma. The soma is the neuronal cell body that, aside from acting as metabolic and genetic center, also processes dendritic input. If input exceeds a certain threshold, the cell will initiate signal output at the base of the axon. The output signal propagates down the axon which arborizes and ends in presynaptic terminals. These terminals contiguously connect neurons for intercellular signal transmission in structures called synapses. Transmitting neurons are referred to as presynaptic and receiving neurons as postsynaptic. That is to say, neuronal signals flow

from presynaptic axons to postsynaptic dendrites[1]. Signal initiation and transmission is facilitated by electrochemical changes in the neuron [1].

2.1.1 Electrochemical dynamics of neurons

Neurons have a membrane potential, E_m (V), due to differences in intra- and extracellular ion concentrations (see Figure 2). Relative to the extracellular fluid, the cytosol is slightly negative.

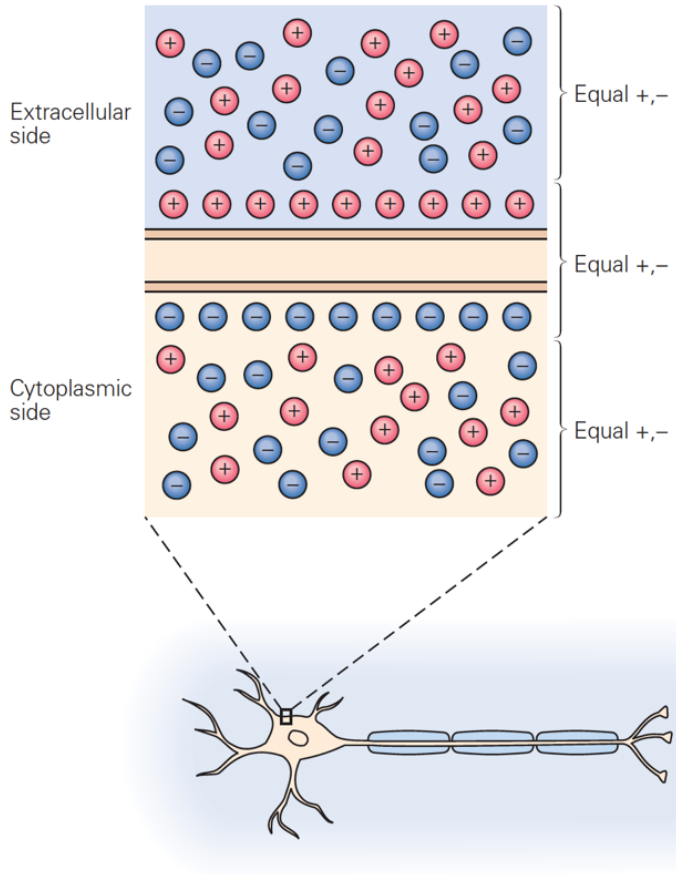

Figure 2 Generalized representation of ion content on the cytoplasmic and extracellular side of a neuron. Blue circles are anions, red circles are cations. The extracellular liquid is positively charged relative to the cytosol due to differences in ion concentrations [1].

The membrane potential can be modelled through the Goldman-Hodgkin-Katz voltage equation (or Goldman equation), which estimates the membrane potential for monovalent cations (C^+) and anions (A^-) as:

$$E_m = \frac{RT}{\mathcal{F}} \ln\left(\frac{\sum_i^n P_{C_i^+}[C_i^+]_{out} + \sum_j^m P_{A_j^-}[A_j^-]_{in}}{\sum_i^n P_{C_i^+}[C_i^+]_{in} + \sum_j^m P_{A_i^-}[A_j^-]_{out}}\right), \text{ where } P_X = \frac{D_X}{L} \quad (1)$$

[1] There are, as is often the case in neuroscience, several exceptions to this rule. Many axons project onto cell bodies, forming axosomatic synapses instead of axodendritic ones. In some cases, axons project onto other axons, forming axoaxonic synapses. Finally, self-projecting axons form synapses called autapses [1].

Where R is the ideal gas constant (8.314 $J \cdot K^{-1} \cdot mol^{-1}$), T is temperature (K), $\mathscr{F}$ is Faraday's constant (96485.322 $C \cdot mol^{-1}$), $[X]_{in}$ and $[X]_{out}$ are the intra- and extracellular molar concentrations of ion X, respectively, and P_X ($m \cdot s^{-1}$) is the selectivity (or relative permeability) of ion X as determined by membrane thickness L (m) and its diffusion constant D_X (s^{-1}).

The concentration differences allot each ion their own characteristic electromotive force, which is understood in terms of their reversal potential. Ion X's reversal potential, E_X (V), equals the membrane potential wherein the net flux of ion X in- and out of the cell is zero. The Goldman equation becomes Nernstian when ions have exceptionally high permeance, which allows their reversal potentials to be calculated as:

$$E_X = \begin{cases} \frac{RT}{\mathcal{F}} \ln\left(\frac{[X^+]_{in}}{[X^+]_{out}}\right), & \text{if } X \text{ is cationic} \\ \frac{RT}{\mathcal{F}} \ln\left(\frac{[X^-]_{out}}{[X^-]_{in}}\right), & \text{if } X \text{ is anionic} \end{cases} \tag{1.1}$$

Ion specific currents (A) arise across the membrane due to the inability of E_m to simultaneously assume the reversal potential of each permeable ion. Instead, E_m assumes an intermediate potential between the various reversal potentials.

The stream of ions makes the membrane a conductor, which allows E_m to also be understood in ohmic terms. Current is the net rate flow of electric charge over space and equals voltage (i.e. potential), V, divided by the conductor's resistance, R (Ω), (or multiplied by the conductor's conductance, G (S)), as per Ohm's law:

$$I = \frac{V}{R} = VG \Leftrightarrow V = \frac{I}{G} = IR \Leftrightarrow R = \frac{V}{I} = \frac{1}{G} \tag{2}$$

With an ohmic interpretation, the reversal potential of ion X is equal to the equilibrium potential wherein the ion-specific current for X is zero [1]. From a biophysical perspective, the most relevant ions with respect to E_m are potassium (K^+), sodium (Na^+) and chloride (Cl^-) seen in Table 1 [11].

Table 1 Comparison of relevant extra- and intracellular ion concentrations for typical mammalian neurons, including their respective reversal potential [11].

Ionic species	Intracellular concentration (mM)	Extracellular concentration (mM)	Reversal potential (mV)
Potassium (K^+)	140	5	–80
Sodium (Na^+)	10	145	+60
Chloride (Cl^-)	10	110	–70 to – 65

Neuronal states are largely determined by their membrane potential, of which there are three importantly distinct potentials: (i) the resting potential, in which a neuron is said to be quiescent;

(ii) the action potential (AP), in which a neuron is said to be signaling, active, spiking or firing; and (iii) the graded potential, in which a neuron receives external stimuli.

APs and graded potentials are dynamic events wherein the concentration gradients rapidly and briefly shift from the baseline in small localized areas. By contrast, the resting potential represents the relatively static and global steady-state, or baseline, of the cell.

2.1.1.1 Resting potential: the baseline

The E_m of neurons at rest is called the resting potential. The resting potential is maintained by both passive- and active ion transporters. Active transport is primarily mediated by Na^+/K^+-ATPase, importing 2 K^+ and exporting 3 Na^+ ions at the cost of 1 ATP. Consequently, upholding the resting potential requires constant energy expenditure [1]. In fact, the brain consumes approximately 20% of the total caloric intake of an adult human[2] [12]. Despite active transport, the resting potential is dominated by the ion with the greatest permeability and reversal potential across the membrane. For most cells, neurons included, this is K^+. The resting potential can often be roughly approximated by E_{K+}. For example, the resting potential of a typical human neuron is approximately –70 mV, whereas E_{K+} = –80 mV. Since E_{K+} is the most negative reversal potential of the relevant ions, it also caps how hyperpolarized a cell can become. This comes into play during the final stages of the AP [1].

2.1.1.2 Action potential: the voltage-gated outgoing signal

Neurons generate sodium activated APs to communicate with other cells. Information is encoded in temporal patterns (or sequences) of APs, called spike trains. APs are all-or-nothing signals that propagate down axons with an amplitude of 100 mV and have characteristic temporal profiles with 5 different stages (see Figure 3); (1) resting (2) rising (3) peak/falling (4) undershot and (5) rebounding [13].

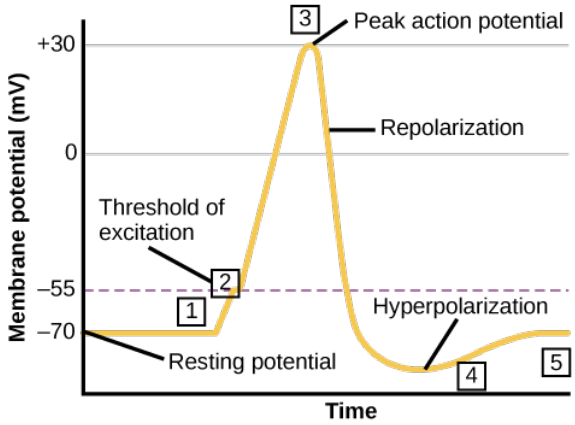

Figure 3 The characteristic temporal profile of an action potential with five distinct stages: (1) resting stage, (2) rising stage, (3) peak/falling stage, (4) undershot stage and (5) rebounding stage. The profile arises due to the interplay between voltage-gated sodium and potassium channels and the extracellular environment further described in the text [14].

[2] An impressive consumption rate considering that the brain makes up less than 2% of total body mass [12]. To put things into perspective, a typical human adult on a 2400 daily caloric intake consumes 100 kcal/hour = 27.8 kcal/s = 116.38 J/s ≈ 116 W. That means that the brain has a power consumption of 23W, slightly less than a 20'' LED-screen. Something to reflect on when sitting in front of your monitor.

The temporal profile, directionality and all-or-none nature of APs arise from the interplay between voltage-gated Na_V and K_V ion channels and the extracellular environment.

The rising stage begins when E_m reaches –55 mV. This is the threshold for activating resting Na_V channels which open up for Na^+ influx, causing rapid depolarization as $E_m \longrightarrow E_{Na+}$. The membrane potential does not reach E_{Na+} since Na_V channels inactivate at +30 mV. Inactivated Na_V channels are, unlike resting Na_V channels, inhibited from opening. This leads to a refractory period wherein new APs cannot be generated, since neurons can only fire again once inactivated Na_V channels recover – making APs one-at-a-time transmissions.

Simultaneous to Na_V channel inactivation, a family of different K_V channels begin to activate leading to dramatic K^+ efflux down its concentration gradient. These events initiate the falling stage, wherein K^+ efflux repolarizes the membrane as $E_m \longrightarrow E_{K+}$. A subset of K_V channels called delayed rectifier potassium channels allow for continued K^+ efflux even in the repolarized state. Because E_{K+} is less than the resting potential, the efflux will hyperpolarize E_m into the undershot stage.

The rebound stage begins when K_V channels begin to close and Na_V channels recover, allowing E_m to return to the resting potential through active transport by Na^+/K^+-ATPases [1].

The propagation of APs depends on Na_V channel distribution. Somatic membranes have <1 Na_V channel per μm^2, whereas initial axon segments have > 160 Na_V channels per μm^2. This high Na_V density facilitates propagation of APs on axons [15]. The refractory period of Na_V channels prevents back-propagation of APs, thus granting neurons directional signaling.

2.1.1.3 Synaptic transmission

Neurotransmitters are chemical messengers that facilitate intercellular communication. This happens when neurotransmitters are released into the synaptic cleft through exocytosis of neurotransmitter-packed synaptic vesicles, called quanta. Although neurotransmitter release can happen randomly, it is most often facilitated by APs.

APs travel down the axon and end at the presynaptic terminal[3], activating local voltage-gated calcium (Ca^{2+}) channels, Ca_V. Activated Ca_V channels cause rapid Ca^{2+} influx that quickly associate with intracellular proteins on vesicles docked and primed near the membrane. Elevated calcium levels enable these proteins to facilitate fusing of vesicles to the membrane-membrane, causing the subsequent exocytosis of neurotransmitters [1, 16].

Once released, neurotransmitters will bind to neuroreceptors on the postsynaptic cell (see Figure 4). The most common excitatory neurotransmitter in the central nervous system (CNS) is glutamate, which primarily interacts with AMPARs.

[3] Unless the axon terminates in an electrical synapse, whereupon the AP is directly conducted to the next cell. These synapses are comparatively rare to the chemical synapse and are largely found in circuits for reflexive defense mechanisms which demand *very* fast responses [1].

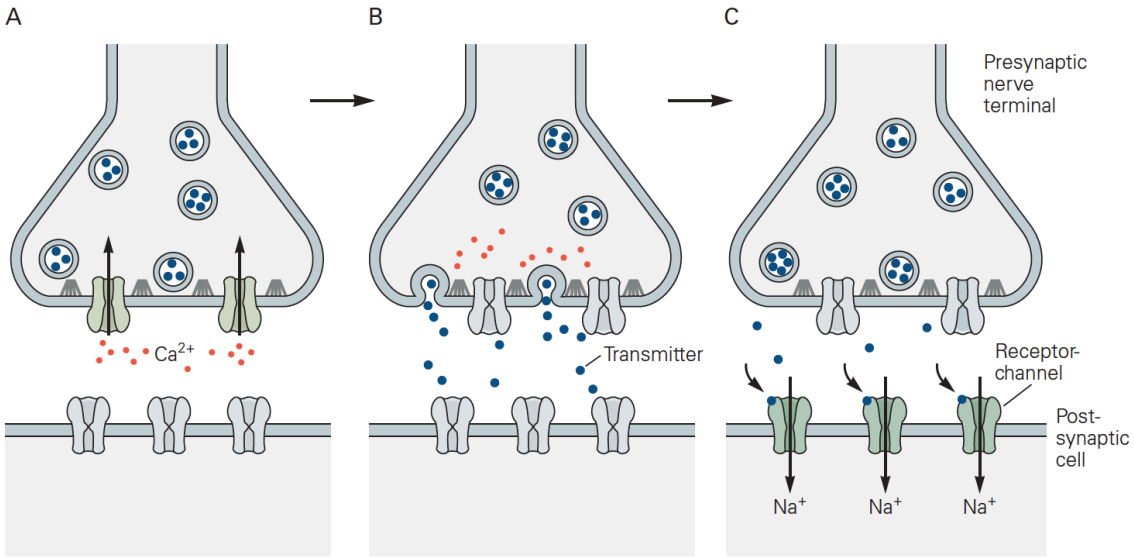

Figure 4 Synaptic transmission: (A) action potential activates voltage-gated calcium channels, causing Ca^{2+} influx, (B) Ca^{2+} associates with docked synaptic vesicles, or quanta, which fuse to the membrane causing exocytosis of neurotransmitters into the synaptic cleft, (C) receptor-channels on postsynaptic cell binds released neuroreceptors, causing influx of receptor-channel specific ions such as Na^{+} [1].

2.1.1.4 AMPARs in the central nervous system

AMPARs are the most abundant excitatory glutamate receptor in the CNS and are ligand-gated ion channels that are enriched at postsynaptic membranes of dendritic spines, where they facilitate and mediate rapid excitatory neurotransmission.

AMPARs are composed of four subunits (GluA1-GluA4) encoded by the genes GRIA1-GRIA4. These subunits usually assemble as dimers-of-dimers into hetero-tetrameric receptors. The receptor is layered in four domains, the extracellular N-terminal (NTD) and ligand-binding domains (LBD), the transmembrane domain (TMD), and the intracellular C-terminal domain (CTD). The domains of the individual subunits are relatively homologous, with the exception of the CTD. The CTD interacts with scaffolding proteins that structure the synapse, and the subunit-diversity in this domain expands the functional range of AMPARs.

The LBD contains four ligand binding sites and requires at least two agonists (e.g. glutamate) to be bound to it in order to activate. Once the LBD is activated, conformational changes in the NTD tugs on and opens the ion-channel in the TMD, generating a depolarizing current. The current is caused by an influx of Na^{+} and Ca^{2+}, and an efflux of K^{+} cations. It should be noted that Ca^{2+} influx is only seen in AMPARs that lack GluA2 subunits [17, 18].

Increasing numbers of agonists bound to the LBD increases the current. When the ion-channel is open, the LBDs of each subunit are set at angles against each other that create an unfavorable and squeezed interface. This interface can rupture within milliseconds, desensitizing the AMPAR by closing the ion-channel and stopping the current. Since the agonists are still complexed with the LBD, the desensitized AMPAR is prevented from further activation until recovery. Signal-strength is thus dependent on the raw number of AMPARs [18-20].

AMPARs are also very dynamic receptors that assemble into nanodomains on the postsynaptic structure. These nanostructures are often colocalized with important scaffolding proteins (e.g. PSD95) and contain up to 20 AMPARs across a ~70 nm span. AMPARs have considerably different kinetics when located within such a nanocluster compared to when they are outside. AMPARs that are clustered are stabilized in their movements whereas outside the structure they diffuse laterally across the membrane surface.

Location of AMPARs in relation to presynaptic glutamate release sites is important for two compounding reasons. First, the local glutamate gradient released by vesicles is limited and transient. Second, AMPARs have poor affinity for glutamate, and only a fraction of exposed AMPARs will be activated upon glutamate release. Consequently, the spatial and temporal dynamics of AMPAR nanodomains has a big impact on the efficiency of signal transmission.

Although AMPAR nanodomains usually remain stable for hours, they can appear/disappear within minutes. The exact mechanisms underlying AMPAR nanodomain dynamics are poorly understood, but of great interest in terms of neuroplasticity (see Section 2.5) [21].

2.1.1.5 Graded potential: the ligand-gated incoming signal

Aside from glutamate and AMPARs, there are many other different species of neurotransmitters and many different corresponding ligand-gated neuroreceptors. Despite this, there are only two possible outcomes from their binding concerning the postsynaptic neuron's E_m; either it depolarizes, or it hyperpolarizes. This depends on the combined reversal potential of the ions passed through by the neuroreceptor in question.

For this thesis the relevant neuroreceptors are N-methyl-D-aspartate receptors (NMDARs), γ-aminobutyric acid class A receptors ($GABA_A$Rs) and most importantly, AMPARs (see previous section). A quick overview of these receptors can be seen in Table 2 below.

Depolarizing events are called excitatory postsynaptic- potentials (EPSPs) (or currents (EPSCs)) since they bring the resting cell closer to the AP firing threshold of –55 mV. Conversely, hyperpolarizing events are called inhibitory postsynaptic potentials (IPSPs) (or currents (IPSCs)) since they inhibit cell-firing by moving E_m away from the firing threshold.

Both EPSPs and IPSPs constitute graded potentials, which are very different from the exclusively excitatory AP in a number of ways. First, they can happen at many places simultaneously; a consequence of having multiple postsynaptic membrane patches to arise on, as opposed to the singular axon. Secondly, graded potentials are not all-or-none signals but can appear with different amplitudes. These two facts are important for how graded potentials summate (see Figure 5).

Temporal summation occurs if successive PSPs are generated before previous one(s) have dissipated. Spatial summation occurs when PSPs are generated simultaneously at different

synapses. If the summated potentials exceed the Na_V threshold of -55 mV at the initial segment of the axon, then an AP will trigger [1].

Table 2 Properties of relevant neuroreceptors to this work [1]

Receptor	Endogenous agonists	Description	Reversal potential (mV)
AMPAR	glutamate	Excitatory non-selective cation channel; causes Na^+ and Ca^{2+} influx and K^+ efflux. Calcium influx is dependent on AMPAR subunit composition.	~0
NMDAR	glutamate + glycine *or* D-serine	Excitatory non-selective cation channel; causes Na^+ and Ca^{2+} influx and K+ efflux. Channel opening is also voltage dependent†. Requires both glutamate and glycine or D-serine.	~0
$GABA_AR$	γ-aminobutyric acid	Inhibitory selective anion channel; causes Cl^- and HCO_3^- influx.	–70 to –65

† The gating mechanism is caused by Mg^{2+} binding to a site in the NMDAR pore, effectively plugging it. Upon depolarization electrostatic forces expel the Mg^{2+} plug. This is interesting since most voltage-gated receptors are gated on the intracellular side [1].

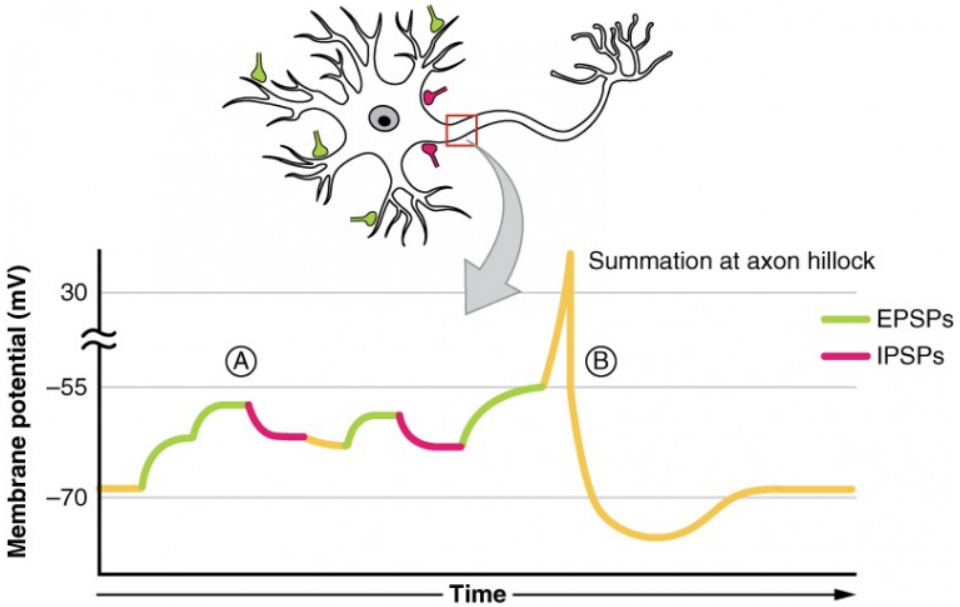

Figure 5 Illustration of summation of excitatory- (green) and inhibitory (red) postsynaptic potentials (E/IPSPs): (A) temporal and spatial summation of E/IPSPs cause the membrane potential to fluctuate, (B) an action potential is generated once summation exceeds the threshold value of -55 mV at the axon hillock [22].

The smallest amplitude is called the quantal amplitude and corresponds to the response elicited by a single quantum. These amplitudes are primarily seen in miniature excitatory/inhibitory postsynaptic currents (mE/IPSCs) which are a subset of spontaneous excitatory/inhibitory postsynaptic currents (sE/IPSCs). Both mE/PISCs and sE/IPSCs are defined as spontaneously arising events (i.e., not produced through artificial/experimental stimuli) and differ from each

other in that sE/IPSCs includes both AP-driven and random neurotransmitter-release events whereas mE/PISCs only includes the latter [23].

Presynaptic influence on quantal amplitude size arises due to heterogeneity in synaptic vesicle size (ø 39.5 ± 5.1 nm), and not because of variability in packed neurotransmitter concentrations which is thought to be homogenous across vesicles [16]. On the postsynaptic side the quantal amplitude is influenced by receptor abundance and dynamics. The quantal amplitude is important in determining synaptic strength, a useful measure of synaptic function especially with respect to neuroplasticity. Functionally, synaptic strength is the averaged responsive change of current or voltage in the postsynaptic neuron produced by activity in the presynaptic neuron. This can also be described for a single synapse as the following product:

$$\text{Synaptic strength} = p_r nq \tag{3}$$

Where p_r is the presynaptic release probability, n is the number of release sites, and q is the quantal amplitude [24].

Taken together, APs and graded potentials show the activity of individual neurons. This activity propagates since neurons are connected in networks. As such, macroscopic activity in neural ensembles or circuits becomes an emergent property. Macroscopic activity in these circuits produce oscillatory patterns that can be at different frequencies than the firing rates of individual neurons [1]. It is thus important to remember that the brain operates on both the macroscopic and microscopic level. The study of electrical activity on either level belongs to the domain of electrophysiology.

2.2 Electrophysiology

Electrophysiology has, for understandable reasons, always been a cornerstone of neuroscience. In the late 1970's Erwin Neher and Bert Sakmann developed a technique called the patch clamp through which electrophysiological properties of individual ion channels could be studied. The patch clamp technique quickly became an indispensable tool for neuroscientists, and in 1991 Neher and Sakmann were awarded the Nobel Prize in Physiology or Medicine[4] for "their discoveries concerning the function of single ion channels in cells" [25, 26]. The patch clamp technique is central to this thesis.

2.2.1 The patch clamp technique

Patch clamping refers to imposing a defined voltage (voltage-clamping, VC) or current (current-clamping, CC) upon a small area of cell membrane, or "patch". The two configurations, VC and CC, allow for precise measurements on current through- and voltage across the cell membrane, respectively. Mechanically, the technique consists in *gently* pushing a ~1 μm-diameter glass micropipette tip filled with suitable electrolyte solution towards a cell

[4] The 20th century was an incredible era for science in general, including neuroscience. Between 1906 and 2014 a total of 17 Nobel Prizes have been shared by 40 laureates working in the field of neuroscience [26].

[27]. Applying light suction to the pipette forces the cell-membrane to bleb into the pipette tip, where denaturation of protruding proteins and extraction of lipids against the inner glass wall causes the membrane to fuse to the pipette thus forming a tight seal. This seal is called a gigaseal due to the rapid climb of electrical resistance from below 10 MΩ to >1 GΩ.

The gigaseal reduces current noise so significantly that picoamp currents of single ion channels can be measured. Indeed, it is through the gigaseal that Neher and Sakmann revolutionized electrophysiology and earned their Nobel prize [28, 29].

Although conceptually simple, the patch clamp technique is often difficult to master and requires ample practice and a fully functioning rig. A modern electrophysiology rig equipped for patch clamping (see Figure 6) usually includes: a recording microelectrode (upon which the micropipette is placed) and a reference electrode; an amplifier (containing or connected to a digitizer) needed to detect and amplify weak signals as well as impose the VC or CC configurations; a head-stage, with stabilizing electrode holders connected to the amplifier; a recording chamber, where the sample or tissue can be placed; microfluidics system for passing artificial cerebrospinal fluid (aCSF) in/out of the recording chamber; micromanipulators and microdrive for fine movements of the micropipette in the x, y, and z axes such that it can be placed upon a neuron; a microscope with sufficient magnification power to resolve individual cells in the recording chamber; a computer with virtual oscilloscopes for visualizing and storing data output; vibration isolation systems, usually in the form of an air table; and a Faraday cage to block external electrical interferences and noise [29].

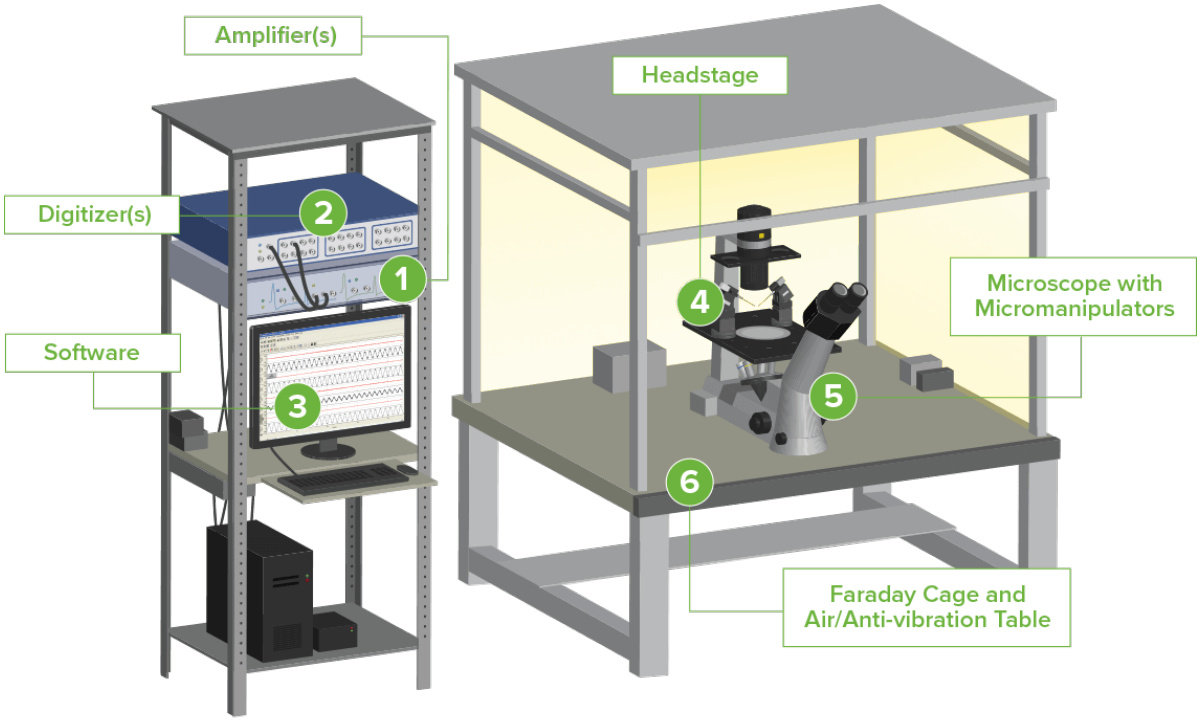

Figure 6 Generalized schematic of an electrophysiology rig: (1) amplifier(s), (2) digitizer(s), (3) software with virtual oscilloscope, (4) headstage with recording chamber, (5) microscope and micromanipulators, (6) Faraday cage and anti-vibration table [30].

2.2.1.1 Patch clamp configurations

Maintaining the gigaseal is called the cell-attached patch (CAP) configuration and is useful for looking at single-channel currents on intact cells. Using the CAP as a springboard configuration allowed for the discovery of three other configurations (see Figure 7). If the CAP configured pipette is suddenly pulled away from the cell, the membrane patch can be excised. If done successfully this will establish an inside-out patch (IOP) configuration, thusly called since the cytoplasmic side of the cell-membrane (or inside) is exposed to the extracellular solution (or outside). The IOP configuration is useful in testing intracellular factors on membrane activity by exposing the patch to defined solutions.

If, on the other hand, one does not retract the pipette but rather applies more suction (in pulses) the membrane bleb can rupture into the pipette, which then joins the cytoplasm with the pipette solution. This is called the whole-cell (WC) configuration since the clamping extends into the entire cell, allowing for intracellular events and activity to be monitored. The WC configuration is used in this thesis.

It is possible for the membrane to reseal itself, which will be noticed if the CAP configuration gigaseal reappears. If, however, the pipette is slowly pulled away from the cell in WC configuration such that the resistance increases to ~500 mΩ and then rapidly pulled away from the cell, the outside-out patch (OOP) configuration can be achieved. During this maneuver the cell-membrane is stretched into a thin fiber which then breaks and restructures itself into a vesicle (cytosolic side inward) at the pipette-tip. In a sense, the OOP is a miniature pseudo-version of the WC configuration. The OOP can be used to study smaller populations of channels and effects of rapidly perfusing solutions into the pseudo-mini-cell [28, 29, 31].

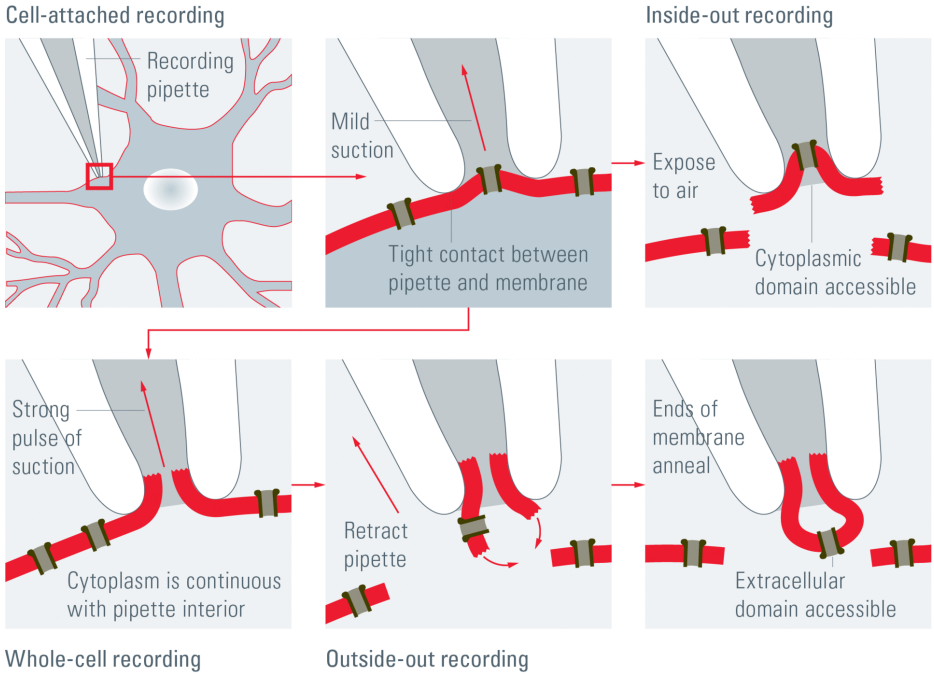

Figure 7 Diagram of the 4 patch clamp configurations. First configuration is the cell-attatched patch (CAP) (top middle). The inside-out patch (IOP) configuration (top right) is achieved from CAP by retracting the pipette. The whole-cell (WC) configuration (bottom left) is achieved from CAP by applying pulses of suction. The outside-out patch (OOP) configuration (bottom right) is achieved from WC by slowly retracting the pipette [32].

2.2.1.2 Electrical equivalent circuit model of patch clamping

Patch clamping is primarily an electrical technique where voltage (or current) induced changes are constantly monitored to assure that the patch clamping is proceeding as planned. Understanding the patch clamp procedure (see Figure 8a) in terms of an electrical equivalent ERC circuit model (see Figure 8b) consisting of batteries (E), resistors (R), and capacitors (C), can be very useful when continuously conceptualizing what the measurements actually mean [1, 27]. The voltage source in this model is the patch clamp (PC) amplifier, E_{PC}, which is in series with the resistor R_{PC}. Both E_{PC} and R_{PC} are shunted by the input capacitance C_{PC}. All potentials (E_{PC}, V_{Pip}, E_m) are measured (or defined) in reference to the ground electrode which is placed in the extracellular solution.

Upon entering the grounded bath, the recording pipette (Pip) immediately gains resistance R_{Pip} and capacitance C_{Pip}. Submerging the pipette into the bath can be understood in the ECR model as closing a double switch (S), S_{CPip} and S_{RPip}. R_{Pip} alters upon approaching the cell, since the solution in the immediate vicinity of the cell is different from the ground electrode.

When gigasealing (seal), the direct connection to the reference electrode is replaced with R_{seal}. Entering the CAP configuration closes the pipette off from the bath solution and through the cell arises a new parallel resistance of R_{CAP}, which can be understood as switching off S_{seal}.

Applying suction pulses to enter the WC configuration will replace R_{CAP} with the much lower access (Acc) resistance, R_{Acc}. The resistance will now noticeably include R_{Pip}, but since the resistances are in series their relationship is simply additive $R_S = R_{Pip} + R_{Acc}$. This can be understood as switching on S_{Acc}, which short-circuits R_{CAP} with R_{Acc}. Switching on S_{Acc} creates a circuit through the cell with the membrane's (m) own potential E_m, resistance R_m and capacitance C_m.

Although a tight seal is formed, there is still leakage of ions from the pipette into the bath through the seal. This causes the problem of leak current seen in the VC configuration, where current is variable (as opposed to CC). A high resistance obtained from a proper gigaseal minimizes this leak current [27].

During patch clamp experiments, cells can be excited/inhibited by stimulating electrodes that produce for example stepwise current injections. In order to do this, the stimulating electrode needs to be placed within a certain proximity of the target cell simply because electrical stimulation acts nonspecifically on cells proximal to the electrode. This is a drawback, both in the sense that the effects are highly dependent on stimulation parameters, but also due to the intrusive nature of placing an auxiliary electrode close to the cell (inside tissue). Recent advances in gene-technology have provided new ways of manipulating cells that sidestep these issues [33].

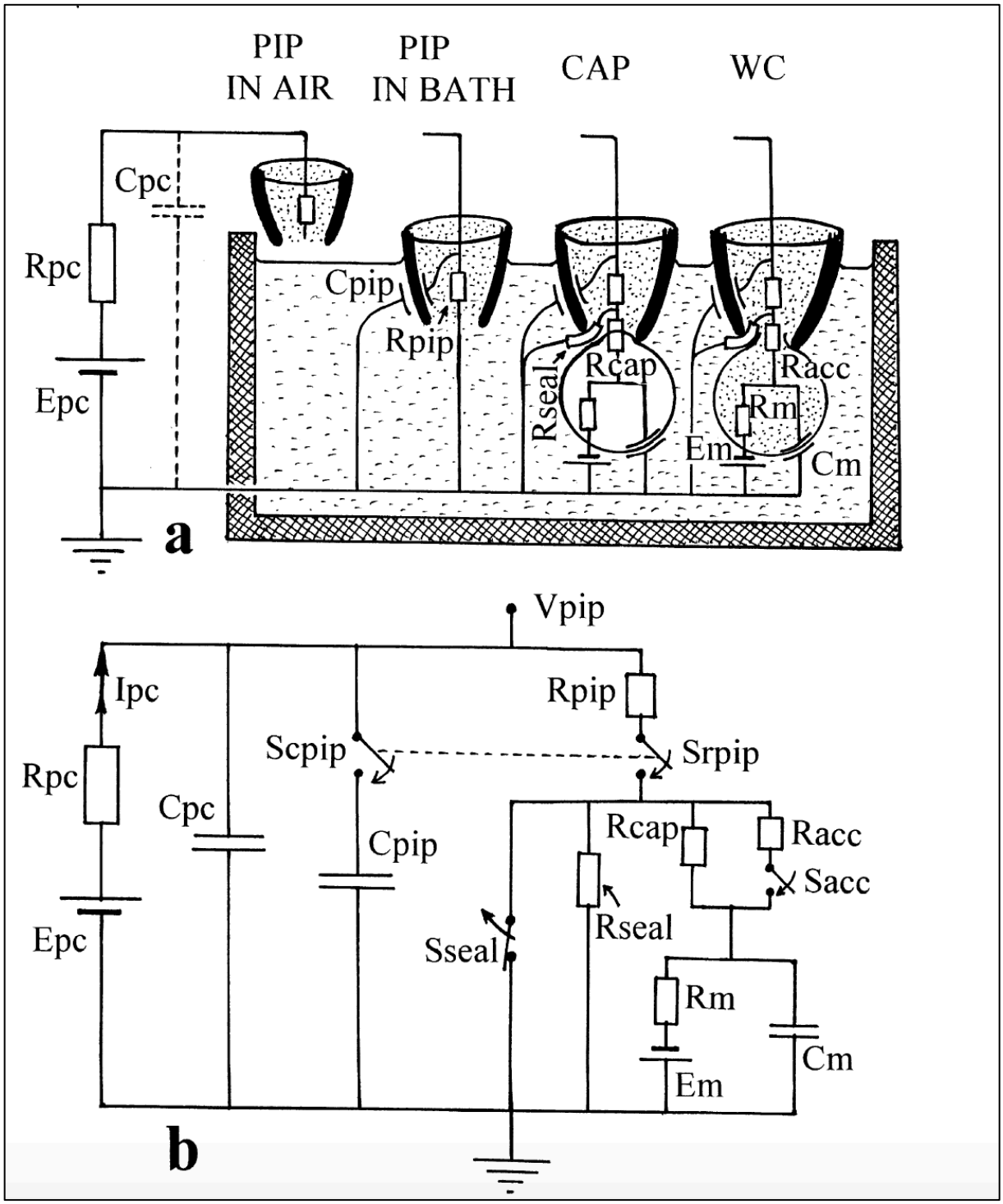

Figure 8 The successive patch clamp procedures for obtaining the whole-cell configuration as modelled by electrical circuit. First a micropipette (attached to the recording electrode) enters the bath, then it forms a giga seal before rupturing the cell-membrane to establish the WC configuration. Part (a) shows the position of the pipette in relation to the cell at various stages corresponding to the abstracted ECR circuit seen in part (b), which represents physical configurations as circuit board switches. The procedure is further explained in the text [33].

2.3 Optogenetics

Optogenetics encompasses a cellular modulation technique wherein exogenous light-sensitive proteins (ion channels and ion pumps) are expressed in cells to make them susceptible to light stimulation [34]. Using optogenetics, cells can be stimulated simply by shining light on them – in stark contrast to the intrusive regime necessary in electrical stimulation.

The first successful use of optogenetics was reported in 2002, where a system composed of three genes from *Drosophila melanogaster* were expressed in mammalian neurons for generation of APs [35]. Research on algae later revealed channelrhodopsins, ion-channels (or pumps) possessing a light-sensitive domain, which could act as single-component optogenetic actuators. This discovery revolutionized optogenetics since single-component systems are considerably easier to employ.

2.3.1 Channelrhodopsins

The first use of single-component optogenetics was published in 2005 where the use of channelrhodopsin-2 (ChR2) in mammalian neurons was used to stimulate APs. ChR2 is a gated light-sensitive nonselective cation channel that causes Na^+ and Ca^{2+} influx in response to blue light (450-490 nm). Exposing ChR2 expressing neurons to blue light causes rapid depolarization, which upon breaching the –55 mV threshold triggers an AP in normal fashion. This provides a non-intrusive and rapidly controllable excitatory stimulation mode [36].

Shortly thereafter, inhibitory actuators were developed in the form of halorhodopsins (NpHR). These are selective light-gated Cl^- pumps that activate upon exposure to yellow light (570-610 nm) [37]. Since the optogenetic actuators are activated at different wavelengths, this allows optogenetics to be a multimodal tool, where cells can express both inhibitory and excitatory opsins.

Although optogenetics as a technique has primarily been used in neuroscience it is now quickly expanding to other fields, especially as a control-tool for intracellular signaling cascades [34].

2.3.2 Implementation of optogenetic system and Lox-Cre recombination

Channelrhodopsins or other optogenetic systems can be delivered to cells by a plethora of standard techniques such as transfection, viral transduction, or simply through the creation of transgenic animal lines. By using specific promotors or conditional recombination systems such as Lox-Cre, expression of light-sensitive proteins can be restricted to cells of interest.

Lox-Cre recombination is a site-specific recombination technique facilitated by Cre recombinase proteins that recognize loxP sites. LoxP sites are 34 bp long sequences consisting of two palindromic and symmetrical 13 bp long repeats that flank an asymmetric 8 bp long spacer. The asymmetry of the spacer gives loxP sites directionality [38]. Sequences that are flanked by two loxP sites are referred to as a floxed cassettes.

In this thesis an optogenetic system was created by breeding mice harboring a floxed ChR2-YFP cassette with mice expressing Cre under the Ca2+/calmodulin-dependent protein kinase II (CaMKII) promotor to produce CaMKIICre-ChR2 mice. CaMKII is one of the most abundant proteins found in the brain, especially in hippocampi where it accounts for ~2% of total protein content [39]. It makes particular sense to place Cre under the CaMKII promotor in this work since the patch clamp experiments are done on hippocampal neurons.

2.4 The hippocampal formation

The hippocampal formation is a compound structure in the medial temporal lobe, comprising the dentate gyrus (DG), the hippocampus proper, and the subiculum (see Figure 9). The dentate gyrus is divided in three regions; the outer molecular layer, the middle granule layer, and the inner polymorphic layer. The hippocampus proper or *cornu Ammonis*[5] (CA), is composed of four main subfields CA1, CA2, CA3 and the DG enveloped CA4. The subiculum extends outwards from CA1 towards the entorhinal cortex, which is the main excitatory afferent of the hippocampal formation.

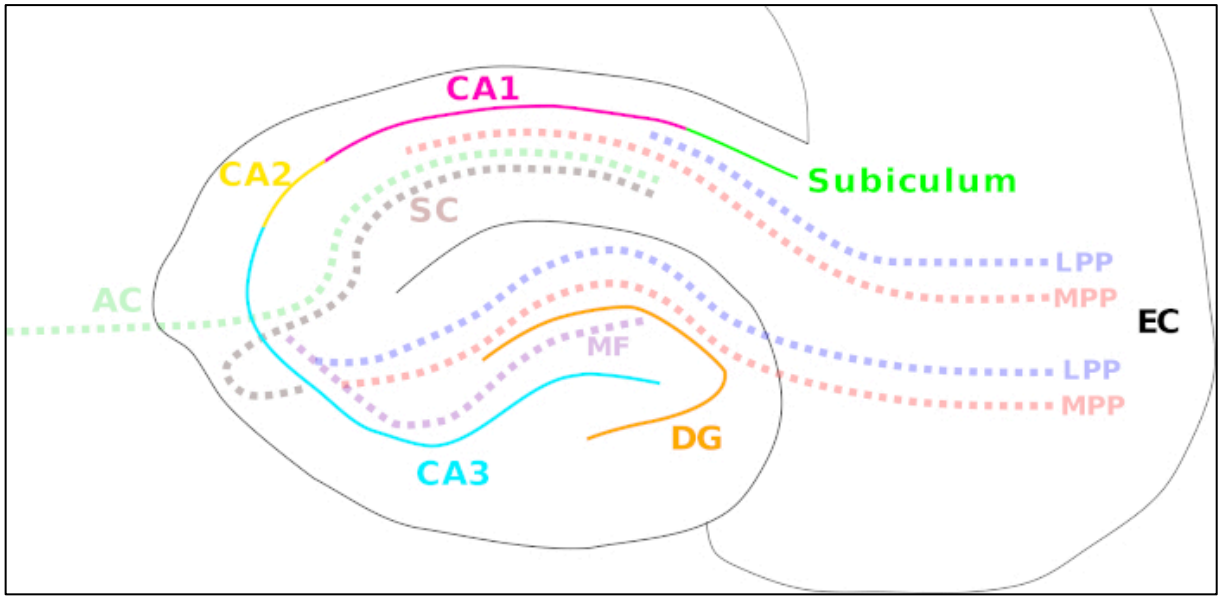

Figure 9 Schematic cartoon of hippocampus outlining different regions (solid lines) and main fiber pathways (dotted lines). Entorhinal cortex (EC, black), dentate gyrus (DG, orange), Cornu Ammonis (CA) extending from subiculum (green) in order: CA1 (magenta) CA2 (yellow) and CA3 (cyan). CA3 overextends, the section that is enveloped by DG is actually CA4. Medial performant path (MPP, red) and lateral performant path (LPP, blue), mossy fiber pathway (MF, violet), Schaffer collateral (SC, brown), and associational commissural pathway (AC, light green) [40].

Pyramidal cells serve as principal cells in the CA and subiculum, whereas granule cells are principal cells in the DG [41]. Pyramidal cells often project their axons to remote regions and are generally large cells with somewhat triangular soma from which apical and basal dendrites sprout. This cellular architecture suggests that the overall role for pyramidal cells is to combine and decide upon functionally diverse inputs from different cell-layers, and to relay this

[5] A linguistic remnant from 16th century anatomical descriptions of the hippocampus, wherein *cornu Ammonis* refers to the horn of the Egyptian god Ammon, or Ammun Kneph. Cornu Ammonis is still used today in its abbreviated form, CA, to describe the hippocampus proper [41].

information via spike trains to the axon-projected region [10]. This suggested role fits well with the central role that CA plays in integrating sensory inputs from various visual, somatosensory, olfactory and auditory cortices [41].

2.4.1 Function of hippocampus

On a functional level, the hippocampus is a key-player in short-term, long-term, and spatial memory consolidation [42]. The hippocampus (and the CA layers in particular) are popular regions for neurophysiological studies. This is not only due to their practically layered anatomical organization, but also because memory (and the loss of it) is of great interest to neuroscience. Although still not completely understood, memory formation is generally thought to involve mechanisms of neuroplasticity such as long-term potentiation (LTP) and depression (LTD). In fact, the first substantial findings on LTP were shown in CA1 cells [43]. Considering that this thesis concerns neuroplasticity investigations, it makes sense to study CA1 cells.

2.5 Neuroplasticity

As stated earlier, the brain's magnificence arises from the contiguous networks that neurons form. Neuroplasticity refers to the nervous system's ability to adapt the structure and function of these networks. This adaptation can happen through apparent morphological changes to brain areas but also through more subtle changes in neuronal biochemistry or synaptic connectivity and strength [44]. Neuroplastic changes to the brain occur throughout life [45]. A prime example of neuroplasticity are the changes made when learning new things. Learning, although not completely understood, involves so called Hebbian forms of plasticity.

2.5.1 Hebbian plasticity

Hebbian plasticity refers to forms of plasticity that align with the Hebbian theory, which states that synaptic strength increases when cells have correlated firing – often summarized in the phrase "*neurons that fire together, wire together*".

There is ample evidence that repeatedly and persistently engaged synapses make both pre- and postsynaptic changes that increase synaptic strength in accordance with Hebbian rule [46]. That active synapses are strengthened, and inactive ones weakened can be seen in many systems that undergo LTP and LTD respectively. However, it should also be noted that overall changes to synapse number are in many systems activity *independent*. As such Hebbian plasticity works by allocation of synaptic resources, not by adding or subtracting them. For a postsynaptic cell a Hebbian plasticity rule can be modelled as:

$$\Delta w_i \propto (x_i - \theta_{x_i})(y - \theta_y) = \begin{cases} > 0, \ if\ x_i > \theta_{x_i}\ and\ y > \theta_y \\ < 0, \ \underbrace{if\ x_i < \theta_{x_i}\ and\ y > \theta_y}_{(a)}, \underbrace{or\ x_i > \theta_{x_i}\ and\ y < \theta_y}_{(b)} \\ 0\ if\ x_i < \theta_{x_i}\ and\ y < \theta_y \end{cases} \quad (4)$$

Where Δw_i is the change of synaptic weight of the i^{th} input, x_i is the activity of the i^{th} input, y is an abstract measure of the postsynaptic cell's activity, and θ_{xi} and θ_y are threshold values for

inducing LTP. If $\Delta w_i > 0$ LTP is induced, whereas if $\Delta w_i < 0$ LTD is induced. LTD can either be heterosynaptic, which happens on inactive synapses by other inputs (condition a); or it can be associative wherein an active synapse fails to produce postsynaptic activity (condition b).

This model can be expanded to include correlation between cells by equaling the postsynaptic cell's activity, y, to the sum of input activities, x_j, multiplied by their respective synaptic weight w_j:

$$y = \sum_j w_j x_j \tag{5}$$

Applying this linear correlation rule to Eq. (4) yields:

$$\Delta w_i \propto \beta + \sum_j \left(\left(x_i - \theta_{x_i} \right) x_j \right) w_j \tag{6}$$

Where β represents all w-independent terms. The latter part of the equation contains the element that correlates the activities of input i and j, which averaged over time can be expressed as the correlation C_{ij} [47]:

$$C_{ij} = \langle \left(x_i - \theta_{x_i} \right) x_j \rangle \tag{7}$$

2.5.1.1 Synaptic competition

Synapses are competitive; meaning that when one synapse strengthens, other synapses weaken. Synaptic competition is necessary to prevent circuits with different functions from wiring together on the same cell. This necessity becomes clear in cases of afferent segregation, wherein independent signaling pathways (e.g., left- and right eye vision) intermix on some layer (e.g., visual cortex) before segregating.

In order for LTD to account for synaptic competition, the anticorrelation must approximately equal the correlation such that $\sum C_{ij} \leq 0$ for all j. In other words, the amount of synaptic strengthening through LTP must equal the loss generated by LTD.

This delicate balance would easily be perturbed by alterations to input patterns or changes in synaptic strength [47]. As such, although LTD provides a means for weakening synapses it is insufficient (or rather, too sensitive) to fully explain synaptic competition [46, 48].

2.5.1.2 Network stability problems

Hebbian learning rules are essentially positive feed-back rules, with two outcomes for network activity: either it drives the pathway towards runaway excitation or total quiescence. This becomes apparent when reviewing Eq (4). Maintaining signal fidelity becomes problematic in such an inherently destabilizing system, as is evident when considering simple signal propagation.

Take, for example, the networks involved in processing visual data, which can be schematized as layers of cells connected by feed-forward links[6]. Here, signal fidelity becomes paramount for higher-order neurons to produce vision corresponding to input received at the photoreceptors. This requires signal gain to be at unity, since gain >1 would recruit more cells and saturate the signal and gain <1 would prevent the signal from even reaching the final layer (see Figure 10). Even if signal gain = 1, such a system would eventually fail if following purely Hebbian rules because activated pathways would potentiate/depress over time [7, 9].

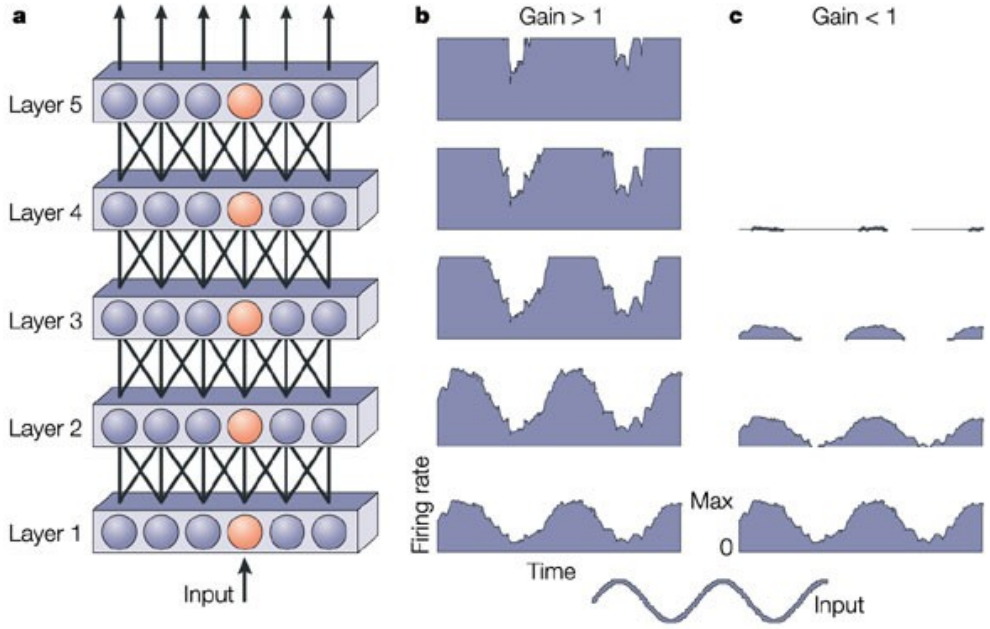

Figure 10 (a) schematic of five network layers connected by feedforward links. Expected output in terms of firing rate of a sinusoidal input: (b) if gain > 1 then each input increases in strength, saturating the signal; (c) if gain <1 then signal fails to propagate to the final layer [7].

2.5.2 Homeostatic plasticity

Hebbian plasticity as a stand-alone model is insufficient to account for synaptic competition [46, 48] and suffers from an inherently destabilizing nature. Indeed, since the first computational models of Hebbian plasticity were made it became apparent that normalizing factors were required to prevent destabilization [7]. These stabilizing factors fit the description of what homeostatic plasticity mechanisms do.

Homeostatic plasticity is a set of physiological mechanisms that regulate brain activity at both network and cellular levels [6]. There are two popular models for homeostatic synaptic plasticity; sliding threshold model and synaptic scaling. The sliding threshold model can be understood as a dynamic function where θ_{xi} and θ_y are modified bidirectionally according to the history of synaptic activity. The consequence of this is that the threshold values for inducing LTP or LTD "slide" in response to sustained activity (or lack thereof) [47].

[6] This is an oversimplified model, signaling pathways are considerably more complex than just layers of feed-forward nodes.

2.5.2.1 Synaptic scaling

Synaptic scaling is a homeostatic plasticity mechanism that works through negative feedback and is known to occur upon long-lasting changes in neuronal activity. It is thought to happen through changes in the raw number of postsynaptic AMPARs on *all* synapses. This contrasts LTP- and LTD-like forms of plasticity, where *individual* synapses are affected.

As a homeostatic plasticity model, synaptic scaling requires that neurons somehow sense their own activity in order to take appropriate action to up- or downregulate towards a set value (see Figure 11). Important to recognize is that the target firing rate must be uniquely set for each individual neuron. This is important as the profile of a neural circuit is determined by the complex interplay of individual neurons; and this interplay is in turn determined by the neuron's unique conductivity and patterns of electric activity. Indeed, if each neuron can uniquely set and regulate their own activity through synaptic scaling, then network stability becomes an emergent property – even in the face of morphological changes and Hebbian plasticity events. Evidence of homeostatic control of firing rate has been seen both *in vitro* and *in vivo* [7, 9, 49]. It is generally thought that this cell-autonomous regulation of firing rate is made possible by calcium-dependent sensors [50].

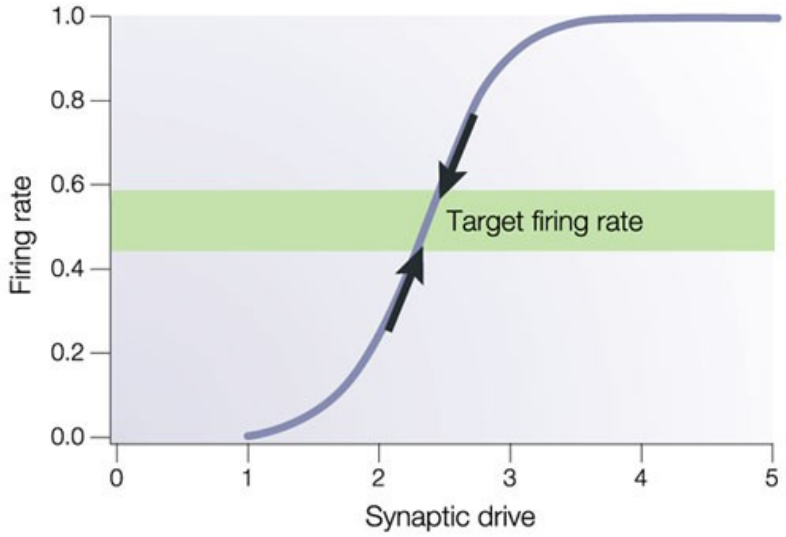

Figure 11 If each cell has its own target firing-rate which they can control through homeostatic mechanisms (arrows) then network stability becomes an emergent property. When synaptic drive increases (through e.g., LTP or other Hebbian forms of plasticity) then firing rate rises; homeostatic mechanisms such as synaptic downscaling (downward arrow) could return the cell to its target firing rate. Conversely, if synaptic drive decreases (through e.g., LTD) then firing rate slower: then synaptic upscaling (upward arrow) could return the cell to its target firing rate [7].

Synaptic scaling is thought to happen in a multiplicative fashion, such that the number of receptors is multiplied by the same factor across all synapses (see Figure 12). As such, each synapse is *scaled* in proportion to their initial strength. Consequently, the relative strength differences (due to e.g., LTP and LTD) between different individual synapses can be preserved while the total excitatory strength is regulated. Interestingly, by linking compensatory changes in overall strength to changes in strength of a subset of inputs – synaptic competition also becomes an emergent property. Synaptic scaling is thus an elegant solution to both problems faced by Hebbian plasticity.

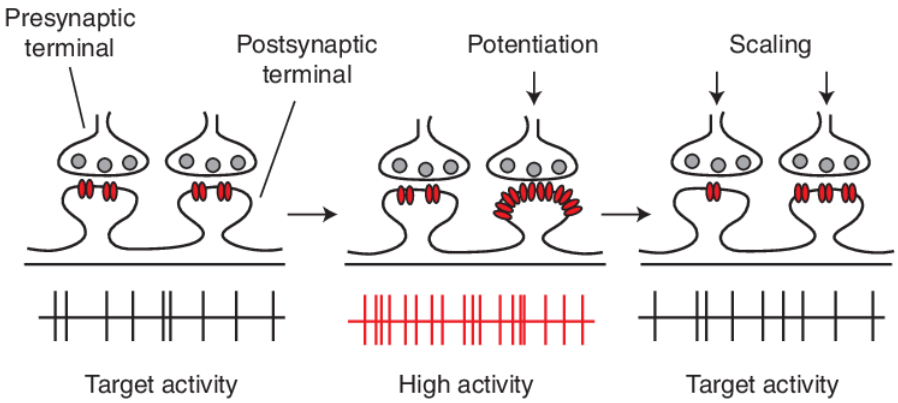

Figure 12 Synaptic scaling contributing to firing rate homeostasis by scaling all synapses by the same factor. Initially the two synapses each have 2 receptors (red ellipses) in an equal 1:1 ratio. When one synapses is potentiated, this ratio becomes 1:3, where the potentiated synapse has 6 receptors and the non-activated synapse remains unaltered with 2 receptors. This leads to high activity, which can be compensated by scaling both receptors. In this scenario the raw number of postsynaptic receptors are downscaled by ½, which retains the 1:3 ratio established through potentiation. This preserves the relative strength differences induced by Hebbian mechanisms. It should also be noted that synaptic competition becomes an emergent property through this type of global homeostatic control. Image modified from [51].

Measuring whether synaptic scaling takes place in such a multiplicative fashion requires that the measured quantity accurately reflects changes across all synapses in the neuron. This can be done by measuring mEPSCs (or sEPSCs) in the WC configuration. Although the strength of an mEPSC amplitude differs between individual synapses, the summed average of mEPSC amplitudes reflect the general excitability of the cell.

Experimentally, synaptic scaling has only been seen to produce measurable changes in synaptic strength after long periods (hours) of altered activity. The reasoning behind this slowness is that rapid forms of homeostatic plasticity might endanger rapid changes in activity needed for neuronal communication. However, in order for homeostatic plasticity (of which synaptic scaling is *one* mechanism) to work it *must* be quick enough to keep up with destabilizing forms of plasticity. It is currently unknown how quickly destabilizing forms of plasticity accumulate in any cell [7, 9]. It is therefore interesting to see if synaptic scaling works differently when modelling pathologies of network instability such as epilepsy.

2.6 Epilepsy

Epilepsy is a spectrum of disorders whose defining feature is the recurrence of seizures. It should be noted that seizures and epilepsy are not interchangeable terms; seizures are *symptoms* and epilepsy is a *disease* wherein seizures are recurrent. Approximately 10% of people will experience one or more seizures in their life, whereas 1-3% will at some point be affected by epilepsy [52]. Epilepsy has a diverse etiology and can be caused by anything from cancer to stroke; the development of hyperexcitable networks that cause epilepsy (epileptogenesis) is a field of intense research [53].

Seizures are generally caused by excessive and abnormally synchronized neuronal firing. When thinking of seizures, people likely think of the convulsive generalized tonic-clonic seizure.

Although easy to recognize, this is not the only way for seizures to manifest. How seizures manifest depends on the location and extent of the involved neurons. Activity originating in bilateral neuron networks are known as *generalized seizures*, whereas seizures starting in unilateral brain regions are known as *focal seizures*. Generalized seizures can manifest themselves (aside from the well-known tonic-clonic seizure) as absence seizures, or as tonic-, clonic-, myoclonic-, or atonic seizures. Clinical features of focal seizures similarly depend on where (and how) in the brain they happen. In the frontal lobe, for example, a seizure can cause wave-like sensations in the head whereas in the temporal lobe, feelings of déjà vu can be elicited; in the parietal lobe, numbness; and in the occipital lobe, hallucinations [4, 6, 8]. Diversity in the clinical features of seizures account for how some people can lead relatively uncomplicated lives with epilepsy – and others not [54].

To better understand epilepsy, it can be helpful to think of the brain as a complex dynamic system that can assume many different states in a multidimensional phase space. The dimensions (e.g., anatomy, cell- and synapse morphology, genetics, and circuit dynamics) of the brain phase space are highly correlated to one another yet have widely different temporal dynamics [55]. The healthy brain generally operates within certain boundaries of functional phase-space regions. In epilepsy however, the brain crosses these boundaries more frequently, resulting in recurrent seizures.

Within this conceptual framework, epileptogenesis can be understood as various attractors situated outside healthy phase-space boundaries, which can aptly be called *seizure space*. With this in mind, it seems likely that the intrinsic mechanisms the brain employs to counter detrimental effects during epileptogenesis are different from how it deals with the chronic phase of epilepsy. To keep a brain from entering (and/or exiting) seizure space requires a set of homeostatic plasticity mechanisms. Interestingly, how homeostatic systems work once epilepsy is established remains unclear. Indeed, homeostatic mechanisms should, in theory, bring hyperexcitable networks back to physiologically healthy spaces; something that is not seen in rodent models nor in patients. The reason why is still unclear [6].

3. Methods

3.1 Animals

Experiments were conducted on CaMKIICre-ChR2 mice that were generated by crossing homozygote CaMKIICre mice with homozygote ChR2 inducible mice. All mice were housed in a 12/12-h light cycle with *ad libitum* access to water and food. Postnatal CaMKIICre-ChR2 mice week 5-7 were used for preparing acute slices.

The work was done under ethics permit 02998-2020. All experiments were conducted according to international guidelines on the use of experimental animals, as well as the Swedish Animal Welfare Agency guidelines, and were approved by the local Ethical Committee for Experimental Animals. This study was carried out in accordance with the recommendations of European Union and the Swedish Board of Agriculture. The protocol was approved by the Swedish Board of Agriculture.

3.2 Acute hippocampal slice preparation

Mice were briefly anesthetized with isofluorane before decapitation. The head was quickly and briefly immersed in chilled sucrose-based cutting solution, containing (in mM): sucrose 75, NaCl 67, $NaHCO_3$ 26, glucose 25, KCl 2.5, NaH_2PO_4 1.25, $CaCl_2$ 0.5, $MgCl_2$ 7 (pH 7.4, osmolarity 305–310 mOsm) before extracting the brain within 2 minutes. The brain was then placed in a Sylgard-coated petri dish containing chilled sucrose-based solution, where the cerebellum was cut and discarded. After this, the entire brain was glued dorsal side down onto a pedestal before being transferred to a cutting chamber containing sucrose-based solution maintained at 2–4°C and constantly oxygenated with carbogen (95% O_2/5% CO_2). Transverse slices of 400 µm thickness, comprising the hippocampi and entorhinal cortex, were cut on a vibrating microtome (VT1200S, Leica Microsystems, advancing speed: 0.03 mm/s and amplitude: 1.3 mm). The hippocampi were separated after slicing, and immediately transferred to an incubation chamber containing sucrose-based solution constantly oxygenated with carbogen (95% O_2/5% CO_2) and maintained at 34°C in a water bath. Slices were allowed to rest for 30 min before being transferred to room temperature and processed for electrophysiology.

3.3 Whole-cell patch clamp recordings

Individual slices were placed in a submerged recording chamber constantly perfused with carbogenated artificial cerebro-spinal fluid (aCSF) containing, in mM: NaCl 119, $NaHCO_3$ 26, glucose 25, KCl 2.5, NaH_2PO_4 1.25, $CaCl_2$ 2.5 and $MgSO_4$ 1.3 (pH 7.4, osmolarity 305–310 mOsm). The temperature in the recording chamber was maintained at 32–34°C.

Recording pipettes (2.5–7 MΩ resistance) were pulled from thick-walled (1.5 mm outer diameter, 0.86 mm inner diameter) borosilicate glass with a Flaming-Brown horizontal puller (P-97, Sutter Instruments, Novato, CA, USA), and contained (in mM): K Gluconate 122.5, KCl 17.5, NaCl 8, KOH-HEPES 10, KOH-EGTA 0.2, MgATP 2, Na_3GTP 0.3 (pH 7.2–7.4, mOsm 300–310). Biocytin (3–5 mg/ml) was added to the pipette solution on the day of recording.

Recordings typically lasted 35 min and cells were held at −70 mV in voltage clamp and at 0 pA in current clamp recordings. Firing pattern was investigated by applying a single 1 s, 500–1000 pA depolarizing current step prior to initiating the optogenetic stimulation protocol (see Section 3.4). After patch clamp recordings the pipette was withdrawn to establish the OOP configuration. After this, the slices were quickly fixed in 4% paraformaldehyde solution in PB buffer for 12–24 hours before being rinsed with potassium phosphate buffered saline (KPBS), and then stored in Walter's antifreeze medium at –10 °C.

Data were sampled at 20 kHz with an EPC-10 amplifier (HEKA Elektronik, Lambrecht, Germany) and stored on a PC computer using PatchMaster software (HEKA) for offline analysis.

3.4 Optogenetic stimulation

After WC configuration was established with leak current <100 pA and normal firing behavior witnessed, the optogenetic stimulation protocol was initiated (see Figure 13). The stimulation protocol consisted in an initial 5 mV test pulse (TP), followed by a continuous recording in VC for 3 minutes. This was to establish the baseline (BL) recording prior to stimulation, which consists in 10 second trains with application of light at 10 Hz frequency, followed by 3 minutes of VC recording and then a TP. The 10 s 10 Hz stimulation resembles a rapid kindling paradigm model popular in epilepsy research [56]. The stimulation was repeated a total of 6 times, yielding six post-stimulation recordings (R1-R6). Light for stimulation experiments were conducted using a 460 nm wavelength LED light source (Prizmatix, Modiin Ilite, Israel). Controls were conducted using a 595 nm wavelength LED light source (Prizmatix, Modiin Ilite, Israel).

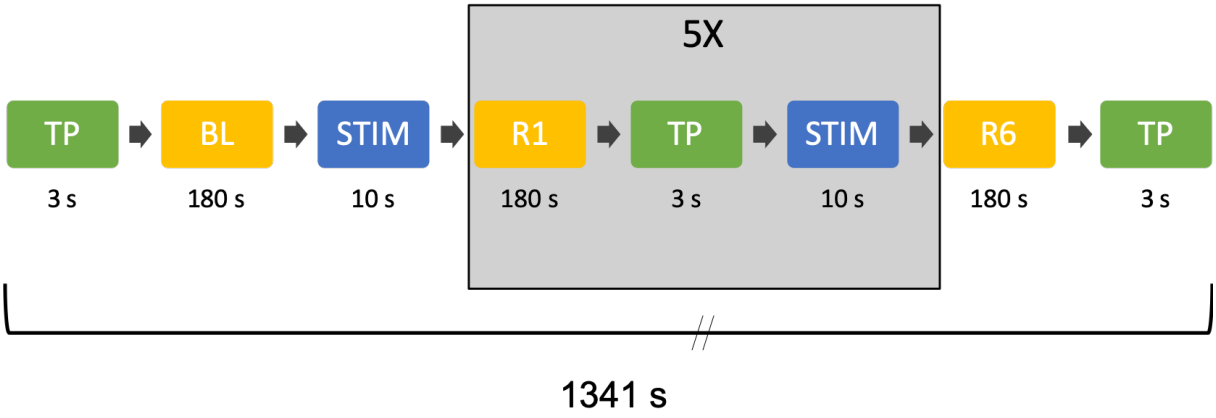

Figure 13 Schematic of optogenetic stimulation protocol under voltage clamp at –70 mV: 3 s test pulse (TP) followed by 180 s continuous voltage clamp recording (BL) followed by 10 second 10 hz light stimulation (STIM) at 460 nm (for control: 595 nm) followed by 180 s post-stimulation continuous voltage clamp recording R1. Prior to each successive STIM block is a 3 s TP. A total of 6X 180 s post-stimulation continuous voltage clamp recordings are made (R1-R6) in this fashion before ending the protocol with a final 3 s TP. The complete protocol takes 1341 s to run.

3.5 Data analysis

sEPSCs were analyzed using a function (github.com/AMikroulis/xPSC-detection) in Python 3.8.1 through Anaconda 3 for template correlation-based detection of PSCs. This function uses

the normalized cross-correlation coefficients of recordings and the template to return a 0.5 – 0.95 range in 0.05 step increments of the correlation coefficient.

Customized scripts (available upon request) processed these results to autogenerate comparative data between each post-stimulation recording, R1-R6, as compared to the BL on: frequencies, interevent intervals (IEIs), mean amplitudes, and rise times for both individual cells and between cells. Each recording is represented equally within its own group by having the same number of events analyzed (sized by the recording with the lowest number of events). Analysis of variance (ANOVA) between cells and recordings was performed on previously generated data in Excel. TP recordings were analyzed on another customized script (available upon request) to produce data on R_s.

4. Results

Investigating synaptic scaling is usually done by looking at amplitude changes to mEPSCs, which is accomplished by preventing AP generation. This is usually done through the use of tetrodotoxin (TTX), which blocks Na_V channels required for AP generation. However, since we are using optogenetic stimulation to simulate epileptic seizures which requires AP generation, we were prevented from using TTX. Consequently, we instead looked at sEPSCs to investigate if rapid synaptic scaling occurred.

sEPSCs were analyzed using a function for template correlation-based detection of PSCs. Filtering criteria for events were set as: correlation coefficient > 0.6, with 20-80% rise time < 5 ms, half-width at > 20-80% rise time and absolute amplitude > 3 pA. Cells were excluded from analysis if detected events were <150 since the add-on scripts scales each recording after the one with fewest events. For similarly qualitative reasons, cells were excluded if $R_s > 25$ MΩ at start and/or end of recording. Raw data is available upon request. Representative traces of the test pulse and the optogenetic stimulations can be seen in Figure 14 below. Similar representative traces of the investigated VC recordings can be seen in Figure 15 below.

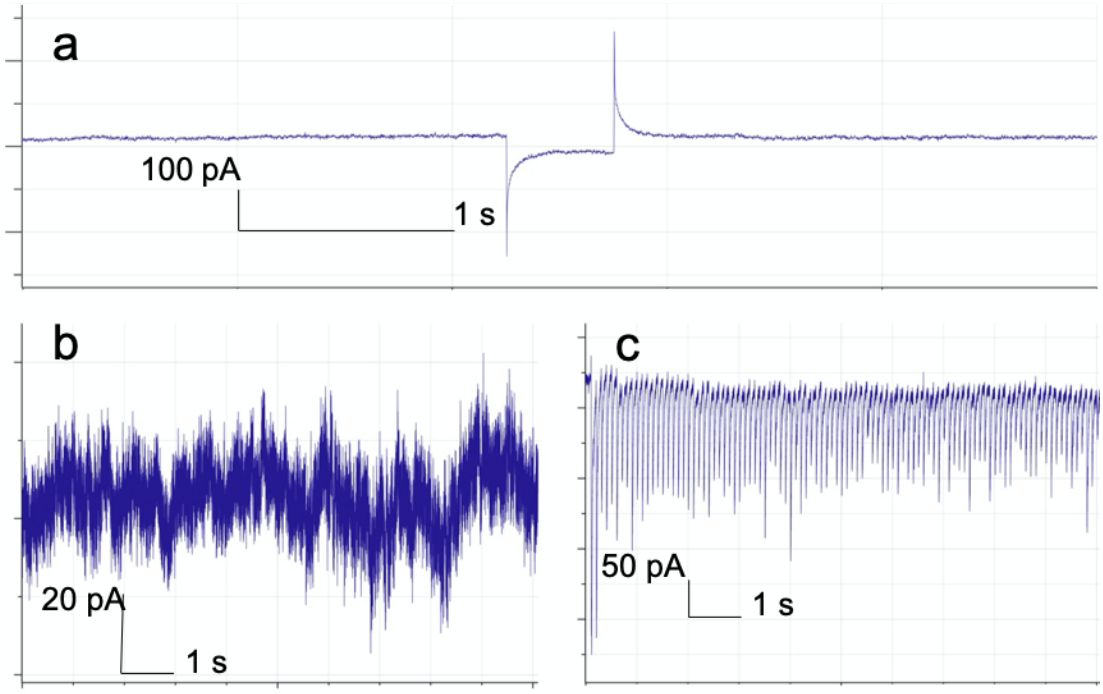

Figure 14 Representative traces of the optogenetic stimulation protocol: (a) test-pulse (TP), (b) stimulation control protocol 595 nm (c) stimulation protocol 460 nm.

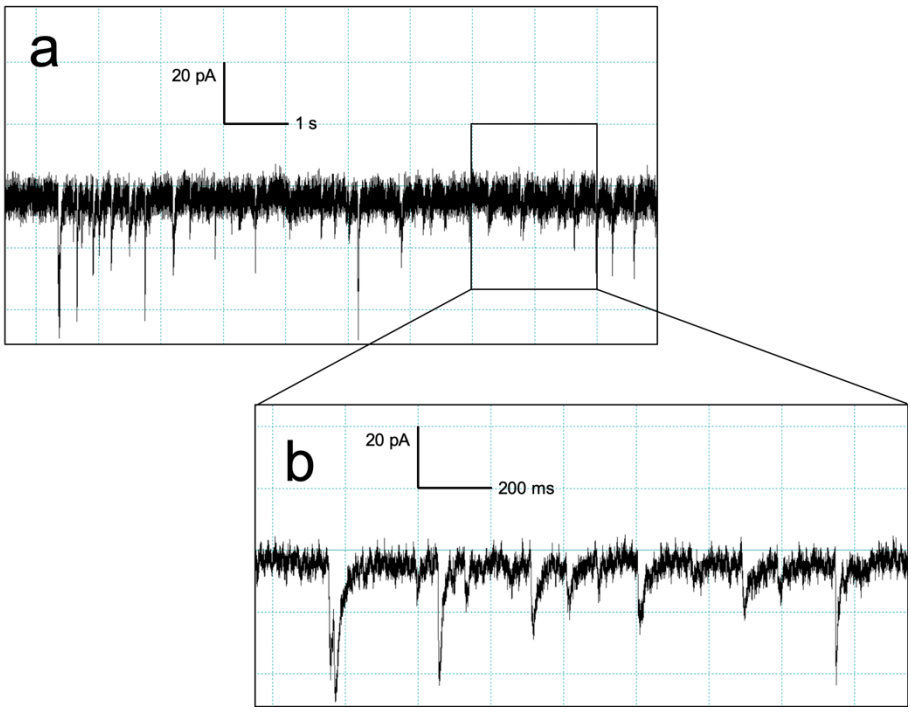

Figure 15 Representative traces of VC recordings. (a) 10 s trace, (b) zoom-in 2 s trace revealing individual sEPSC peaks

First, we looked at whether the distribution of sEPSC amplitudes were altered from the baseline (BL) as compared to the final poststimulation recording (R6) of CA1 pyramidal cells of CAMKIICre-ChR2 mice (n=6) subjected to the voltage clamped optogenetic stimulation protocol (see Section 3.4). However, no significant changes were observed with regards to amplitude distribution before and after stimulation (see Figure 16).

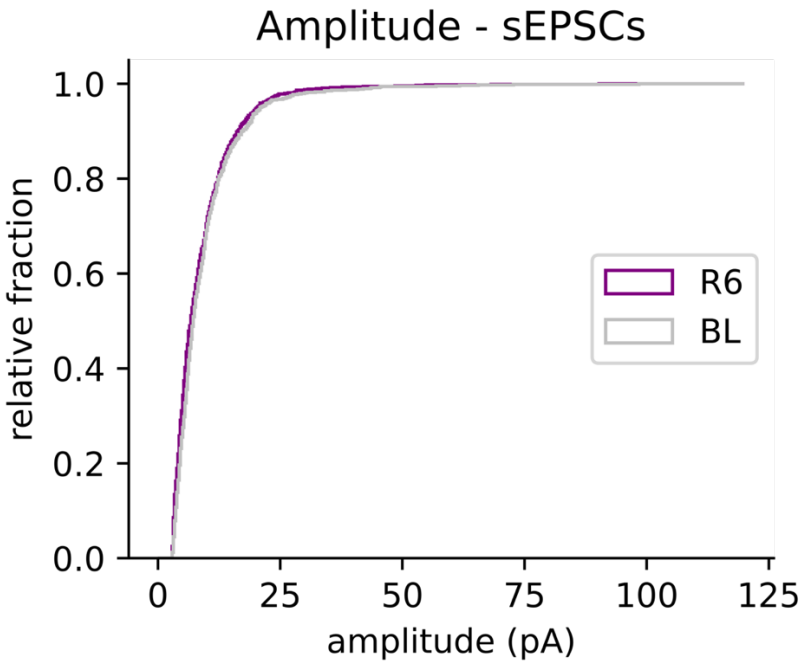

Figure 16 Relative fraction of sEPSC amplitudes (pA) before (BL, gray) and after the final stimulation (R6, purple).

Next we looked at whether there were any significant changes between each individual post-stimulation recording (R1-R6) as compared to the baseline. Again, no significant changes were observed – nor was any clear trend observed (see Figure 17).

Single factor ANOVA (α=0.5, df =6) on the amplitudes between cells in each recording further shows that no significant change has occurred with F = 0.3087 << F_{crit} = 2.3718, and P-value = 0.9282. Single factor ANOVA is a suitable approach to determine since we are looking for changes to the mean between independent groups and independent recordings.

A control experiment was made with similar voltage clamp optogenetic stimulation protocol configuration with the exception of using yellow light at 595 nm, which does not activate ChR2. No changes in mean amplitude were observed here either (see Figure 18), which was expected. Similar single factor ANOVA (α=0.5, df=6) test was run on the control dataset showing no significant difference to the mean either with F = 0.4867 << F_{crit} = 2.8477, and a P-value = 0.8076.

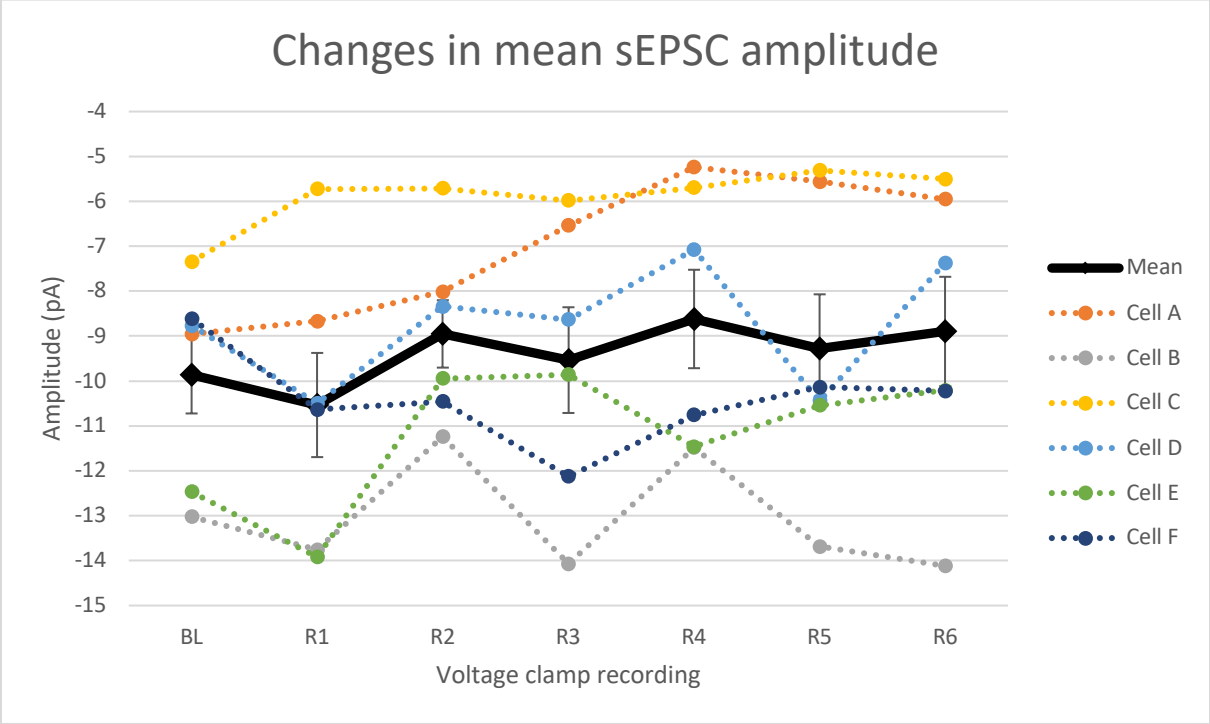

Figure 17 Changes in the mean sEPSC amplitudes (pA) before and after 420 nm optogenetic stimulations for n=6 cells; BL = baseline recording, R1 = recording after 1st stimulation, R2 = recording after 2nd stimulation, R3 = recording after 3rd stimulation, R4 = recording after 4th stimulation, R5 = recording after 5th stimulation, and R6 = recording after 6th stimulation. Solid black line with standard error bars shows the mean of all cells, which reveals no significant change to mean amplitude for each individual post-stimulation recording (R1-R6) as compared to the baseline. Dotted colored lines show mean amplitudes for individual cell recordings, with cell A (orange), cell B (gray), cell C (yellow), cell D (blue), cell E (green), and cell F (dark blue).

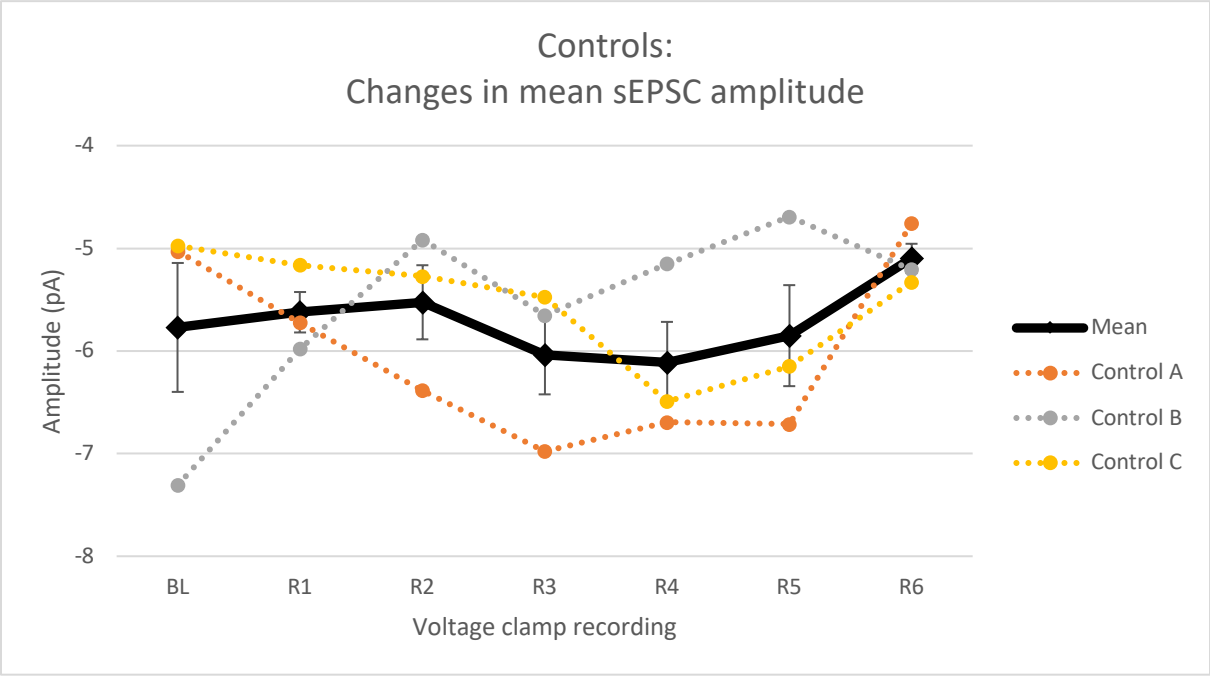

Figure 18 Changes in the mean sEPSC amplitudes (pA)before and after 595 nm optogenetic stimulations for n=3 control cells; BL = baseline recording, R1 = recording after 1st stimulation, R2 = recording after 2nd stimulation, R3 = recording after 3rd stimulation, R4 = recording after 4th stimulation, R5 = recording after 5th stimulation, and R6 = recording after 6th stimulation. Solid black line with standard error bars shows the mean of all cells, which reveals no significant change to mean amplitude for each individual post-stimulation recording as compared to the baseline. Dotted colored lines show mean amplitudes for individual cell recordings, with control cell A (orange), control cell B (gray), control cell C (yellow).

4.1 Changes to sEPSC interevent intervals

In general, changes to PSC amplitude indicate postsynaptic changes whereas changes in frequency relate to changes in presynaptic release mechanisms [57]. Since we did not see any significant changes to sEPSC amplitude, we next investigated if homeostatic control was exerted by presynaptic means instead. This was done by looking at frequency of events, which can be converted to IEIs since IEI simply measures time between peaks.

Interestingly, IEIs did not change significantly throughout the voltage clamped optogenetic stimulation either, as can be seen Figure 19. Single factor ANOVA test (α=0.5, df=6) further supports that no significant change in the IEI mean between groups has occurred, with F = 0.1153 << F_{crit} = 2.3718 and a P-value = 0.9940.

Similarly, the controls did not exhibit any changes to their IEIs (see Figure 20). This was also supported by a similar single factor ANOVA (α=0.5, df=6) between groups, with F = 0.5173 << F_{crit} = 2.8477 and a P-value = 0.7859.

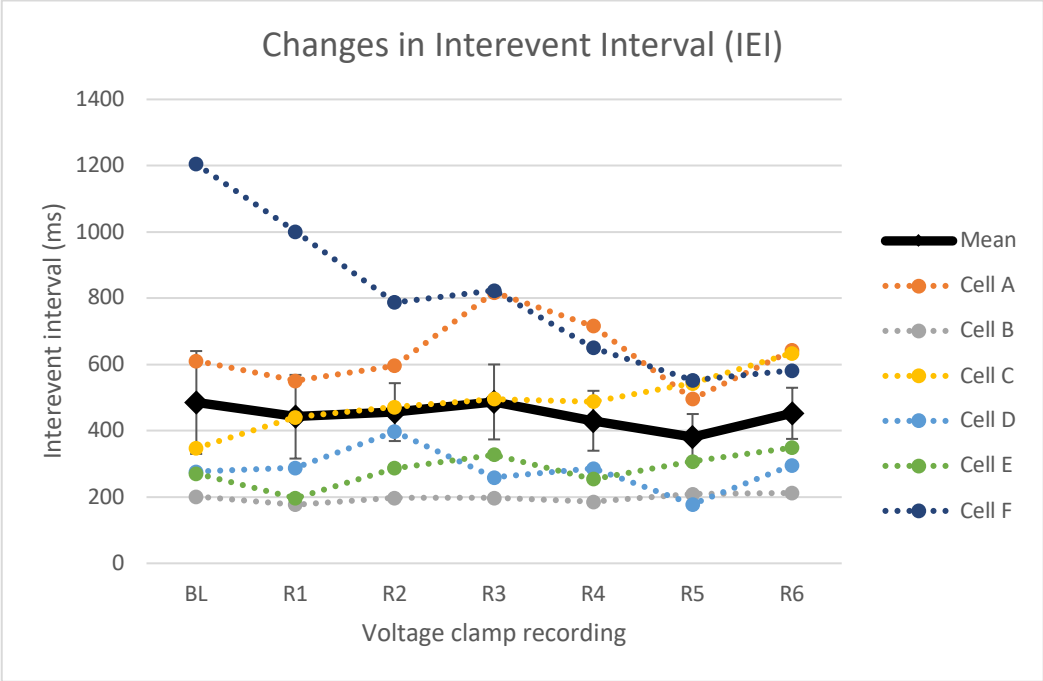

Figure 19 Changes in the mean sEPSC amplitudes (pA) before and after 420 nm optogenetic stimulations for n=6 cells; BL = baseline recording, R1 = recording after 1st stimulation, R2 = recording after 2nd stimulation, R3 = recording after 3rd stimulation, R4 = recording after 4th stimulation, R5 = recording after 5th stimulation, and R6 = recording after 6th stimulation. Solid black line with standard error bars shows the mean of all cells, which reveals no significant change to mean amplitude for each individual post-stimulation recording (R1-R6) as compared to the baseline. Dotted colored lines show mean amplitudes for individual cell recordings, with cell A (orange), cell B (gray), cell C (yellow), cell D (blue), cell E (green), and cell F (dark blue).

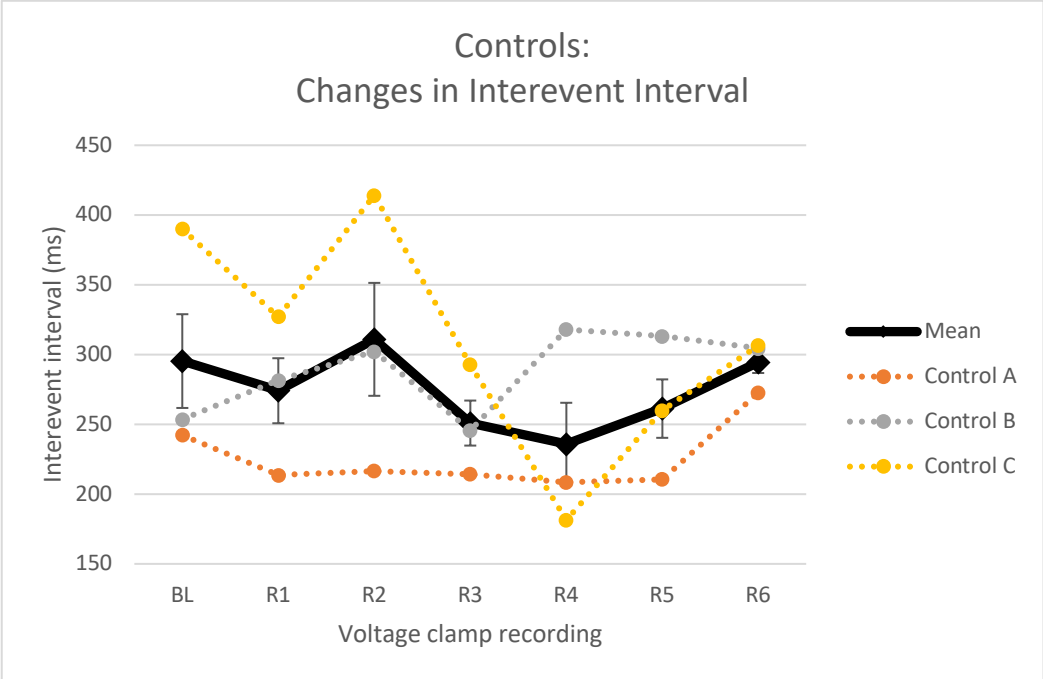

Figure 20 Changes in interevent intervals, IEIs (ms), before and after 595 nm optogenetic stimulations for n=3 control cells; BL = baseline recording, R1 = recording after 1st stimulation, R2 = recording after 2nd stimulation, R3 = recording after 3rd stimulation, R4 = recording after 4th stimulation, R5 = recording after 5th stimulation, and R6 = recording after 6th stimulation. Solid black line with standard error bars shows the mean of all cells, which reveals no significant change to mean amplitude for each individual post-stimulation recording as compared to the baseline. Dotted colored lines show mean amplitudes for individual cell recordings, with control cell A (orange), control cell B (gray), control cell C (yellow).

5. Discussion

Neurons are highly variable. Subsequently this makes patch-clamp experiments highly variable too. Taking the relatively low number of sample cells into account clarifies the difficulty reaching conclusive results. It does however *seem* reasonable to expect that *something* should happen in response to repeated stimulation. It is therefore peculiar that neither pre- nor postsynaptic function seems to have been measurably affected. Although having no effect as outcome is possible, it could also be a result of the experimental design, unforeseen factors and/or confounders.

5.1 Experimental design

5.1.1 Consequences of placing ChR2 under the CaMKII promotor

ChR2 is, as stated earlier (see Section 2.3.1) a gated light-sensitive nonselective cation channel that causes Na^+ and Ca^{2+} influx in response to blue light. We placed this under the CaMKII promotor to ensure high expression-rates, since CaMKII is highly expressed in hippocampal neurons. Through this overexpression ChR2 distributes uniformly throughout the membrane [58]. But this form of overexpression can lead to a confounder with regards to presynaptic action. As stated earlier, synaptic transmission occurs due exocytosis of synaptic vesicles, which in turn occurs when Ca^{2+} binds to proteins on the vesicles. Normally this is facilitated by the AP activating Ca_V channels at presynaptic terminals. In our case we are creating unnaturally high Ca^{2+} influx by introducing an additional Ca-channel in the form of ChR2. What is interesting here is the fact that we still do not see any major changes in presynaptic activity. It seems likely that higher Ca^{2+} influx will deplete the pool of synaptic vesicles quicker, yet this is not seen. Perhaps the optogenetic stimulation hides the presynaptic homeostatic effect, and in a "normal" case (i.e. without added Ca channel at the presynaptic terminal) we *would* see a difference in IEIs.

This problem could be circumvented by somehow ensuring that ChR2 expression becomes localized to the axon initial segment. This has been done previously by adding the ankyrinG-binding loop (found on Na_V channels similarly localized) to the intracellular terminus of the protein. This would have similar effect as the subcellular localization of Na_V has on AP propagation (see Section 2.1.1.2) [58]. Although this would still cause unnatural Ca^{2+} influx at the soma, it is much more similar to the natural means of AP generation than uniform expression. If ChR2 is only expressed at the axon initial segment it will only cause depolarization by AP generation, unlike our case where ChR2 activation causes simultaneous depolarization across the entire cell. The added benefit of this is that the confounder arising from added Ca^{2+} influx at the presynaptic terminal simply disappears.

However, expressing ChR2 with an intracellular ankyrinG-binding loop could come at the experimental "cost" (aside from purely financial costs of employing more advanced gene-constructs) of weakening the impact of optogenetic stimulation. In other words, localizing ChR2 expression removes the "guarantee" that cells will fire in response to light. This highlights how experimental design is often a matter of compromises, rather than solutions.

5.1.2 Consequences of voltage clamping

Although the resting potential for a neuron is often approximately –70 mV, clamping a cell at this potential prevents it from engaging in voltage-dependent activities. This compounds with the issue of globally calcium levels due to the way our optogenetic system is formed. It seems likely that our use of ChR2 will affect all calcium-dependent pathways – and if any of these are voltage-dependent then the VC will disrupt it further. What the effects of these compounding factors might be is not entirely clear.

Perhaps more importantly, VC at –70 mV prevents APs from being generated since this requires breaching the –55 mV threshold. If rapid synaptic scaling is somehow dependent on AP generation, then maintaining the cell at –70 mV between stimulations will hinder that function. That this is the case would be counterintuitive since synaptic scaling experiments are often done in the presence of TTX, precisely in order to prevent APs.

In fact, local perfusion of TTX at the soma has been shown to be sufficient to cause AMPAR upscaling – simply by preventing postsynaptic spiking. Indeed, this project would have employed TTX to study mEPSCs (rather than sEPSCs) if it wouldn't render repeated optogenetic stimulation meaningless. Since sEPSCs are less likely to correspond to the quantal amplitude they provide a less reliable measure on synaptic strength.

However, upscaling and downscaling are not necessarily the same on a functional level. It could also be that rapid synaptic scaling employs different trafficking pathways than "slow" synaptic scaling – and it could be that these pathways are dependent on AP generation. Indeed, evidence suggests that there are different types of synaptic scaling.

For example, the composition of trafficked AMPARs are different when both NMDARs and postsynaptic firing are simultaneously blocked, as opposed to when only postsynaptic firing is blocked. In the latter, coordinated changes to both GluA1-A2 are observed whereas in the former there is a selective increase in GluA1 [50]. The existence of LTP and LTD (and different types of these, too) clearly shows that there is more than one way to influence AMPAR accumulation and trafficking. It is therefore perhaps better to think of synaptic scaling as an outcome, rather than a singular process. In this thesis we are investigating a (potentially) new form of synaptic scaling, which we call rapid synaptic scaling.

5.1.2.1 VC prevents AP generation differently from TTX

Even if synaptic upscaling has been induced by blocking AP generation, how that AP generation is blocked can be of interest. The way TTX prevents APs is through blocking Na_V channels, not by directly manipulating E_m as is done by VC in the current case. As such, a cell exposed to TTX is still susceptible to changes in E_m. Consequently, TTX does not rule out the possibility that synaptic scaling employs certain voltage dependent pathways.

For example, it has been shown that disrupting NMDAR function inhibits threshold sliding in the primary visual cortex of mice [59]. As previously described, NMDARs are partially voltage

gated cation-channels. More specifically, depolarization is needed to repel the extracellular Mg^{2+} plug blocking the NMDAR channel. Since <10% of AMPARs in the hippocampi[7] lack GluA2, most hippocampal AMPARs do not cause Ca^{2+} influx [60]. Consequently, NMDARs play a larger overall role in Ca^{2+} influx.

Considering that the sensors neurons use to regulate their own firing-rate are thought to be calcium dependent, it is tempting to suggest that impaired NMDAR function implies impaired "sensing" abilities. However, receptor trafficking underlying normal synaptic scaling have been independent of NMDAR activation as previously mentioned [7, 49, 50]. The calcium-dependent sensors are thought to be located in the soma, not the dendrite [61]. This is a good reminder on the importance of distinguishing subcellular locations; the neuron is not a homogenous structure.

5.1.3 Space clamping issues

The fact that the neuron is not a homogenous and spherical system has implications for what is actually recorded during voltage-clamping. Because the neuron is non-spherical, the recording electrode is unable to clamp E_m over large distances. This means that some of the currents recorded are originating at places with different membrane potentials. This exemplifies the issue of so-called space clamping; the uncertainty to how far the clamp actually extends.

Direct measures of VC errors in central neurons suggest that somatic VC does not control voltage at apical dendrites – and in fact distort measurements of synaptic inputs in a distance-dependent manner [62, 63]. Because VC does not exert voltage control at apical dendrites, NMDAR function is not necessarily hindered – which is good if rapid synaptic scaling is NMDAR dependent. However, space clamping is not an issue at the soma and the electrode will exert sufficient control to prevent the cell from firing.

5.1.4 Consequences of whole-cell patch clamping

It is important to understand that patch clamping is not an idealized technique (as evidenced by the space-clamping issue), and there is often virtue in examining details surrounding the technique. Since the artificial intracellular solution maintained in the pipette *is* different from the real intracellular solution there will be exchange of molecules once in the WC configuration. This cell dialysis can lead to loss of molecular machinery otherwise important to the biological phenomena being investigated, a difficult problem to circumvent. Indeed, cell functionality is generally inferred from looking at the electrical state of the neuron – from which the state of health can be assessed. If the neuron appears healthy (or sufficiently so), then we assume that most machinery is also working. This is why recordings should be evaluated, not only on the quality of the clamp – but also on cellular health. These two are fortunately correlated in the sense that good clamps are only possible on healthy cells. In the current work quality was upheld by only recording cells with <100 pA in leak current.

[7] Interestingly, the hippocampi are one of the few structures where AMPAR subunit composition has been quantitatively determined [60].

5.1.5 Importance of electrochemical dynamics

There is however another issue that should be assessed with regards to cell dialysis and the VC recordings. It should be recognized that voltage clamping is not achieved by the pipette solution, but rather through the amplifier controlling the electrode. The currents being recorded are, in a sense, the things the amplifier detects that need to be corrected for it to maintain whatever the desired clamp setting is. So, whereas the clamp control is purely electrical the recorded currents/voltages arise electrochemically. As such, although the composition of the artificial intracellular solution does little in terms of controlling the clamp, it will influence the electrochemical dynamics of the neuron.

In the current work, our pipette solution has comparatively high concentrations of complexed chloride species (see Section 3.3). The reversal potential for Cl^- is normally between –70 and –65 mV. Diffusion of the pipette solution into the cytosol will increase the pool of available Cl^- and thus decrease the difference between intra- and extracellular Cl^- concentrations. Consulting Table 1 and applying Eq 1.1 then yields a smaller magnitude for E_{Cl^-}.

Since VC is held at –70 mV > E_{Cl^-}, Cl^- influx will be recognized as a depolarizing and excitatory current. Although the current is depolarizing, it is a mistake to call it excitatory since Cl-channels are generally inhibitory. Indeed, in the current experimental design GABAergic activity is indistinguishable from glutamatergic activity. This is perhaps one of the biggest design flaws since it clouds precisely those measurements that we were interested in. If we were to view the neuron in purely Ohmic terms, then this fact would be difficult to recognize. This highlights the importance of recognizing the chemical driving forces at play in patch clamp experiments.

5.1.6 Summary of potential design flaws

The potential flaws in experimental design hitherto discovered arise from (a) introducing an additional Ca-channel in the form of ChR2 at the presynaptic terminals (b) keeping the cell in VC at –70 mV and in WC configuration, (c) having a pipette solution with high chloride content and (d) not being able to measure mEPSCs.

Introducing an additional Ca-channel in the form of ChR2 causes unnaturally high Ca^{2+} influx at the presynaptic terminals. This in turn causes unnatural conditions for exocytosis of synaptic vesicles.

Keeping the cell in VC at –70 mV prevents voltage dependent neuronal function such as AP generation, which could perhaps be important for rapid synaptic scaling. Due to space clamping it is unlikely that this affects NMDAR function on apical dendrites.

The high chloride content in the pipette solution, combined with keeping VC at –70 mV prevents excitatory and inhibitory activity from being analytically distinguished. This distorts interpretation of sEPSCs amplitudes, but not IEIs.

The point of using optogenetic stimulation is to induce synchronized hyperactivity in all networks to model epileptic seizure. Since TTX would render the entire networks inactive it would defeat the model's purpose. As such we were unable to measure mEPSCs, which more accurately reflect synaptic strengths. However, since we are measuring averages – and since we did not see any change in presynaptic function (evidenced by no change in IEI), it is perhaps not too relevant to measure mEPSCs as opposed to sEPSCs. Indeed, if rapid synaptic scaling occurs as hypothesized then both types of currents should experience a decrease in mean amplitude. However, if the optogenetic model affects presynaptic function by causing unwarranted Ca^{2+} influx it could be worth revisiting presynaptic effects.

5.2 Future experimental design

First and foremost, future experimental design must expand on the sample-size. Going forward it would also be reasonable to do the experimental setup in CC at 0 pA during the stimulations and only entering VC at –70 mV before and after the entire protocol. Such a setup would enable the employ of voltage-dependent pathways, which could be important for rapid synaptic scaling. However, this would be at the loss of understanding the temporal dynamics of rapid synaptic scaling. If possible, it would also be very good to ensure localization of ChR2 expression to the axon initial segment to prevent both pre- and postsynaptic confounders due to raised calcium influx.

One obvious way to resolve GABAergic signals would be to decrease the chloride content such that entering WC configuration actually dilutes the available Cl- pool, driving $E_{Cl^-} > -70$ mV. This would have the added benefit of enabling analysis on changes to inhibitory signaling, which could be another homeostatic control mechanism at play. This should be done carefully to prevent unnecessarily harmful cell dialysis. Another way would be to use drugs that specifically block GABA receptors, such as picrotoxin (PTX) [64]. However, this would also dramatically change normal network behavior. If rapid synaptic scaling occurs, it should occur even in the face of ongoing inhibitory signals. Nonetheless, performing a few experiments with PTX would provide a reference sample that could relate how important it is to distinguish GABAergic signals.

Optogenetics open up exciting new possibilities for experimental design. If inhibitory channelrhodopsins activated at different wavelengths were coexpressed with excitatory ones such as ChR2, then networks could be inhibited between stimulations. Again, it would be good to express this at the axon initial segment. This would allow mEPSCs to be recorded without the use of TTX. Recently, researchers developed an optogenetic system called BiPOLES (Bidirectional Pair of Opsins for Light-induced Excitation and Silencing) which consists of a fusion protein of such a pair of opsins [65]. Using this would remove variability in opsin expression, granting proportionality to the bidirectional optogenetic control of each cell. However, this would again be difficult to implement if rapid synaptic scaling requires voltage-dependent machinery. One benefit of measuring mEPSCs would be the more readily apparent changes in synaptic strength. Indeed, a multiplicative scaling behavior measured with mEPSCs would be immediately recognizable in cumulative distributions as the one seen in Figure 16 -

the same could not be said for sEPSCs, which would include amplitudes arising from multiple quantal loads. This problem could be resolved by increasing sample size, a rather inelegant solution when considering the three R's of animal research. As such, measuring mEPSCs would have the added benefit of requiring a smaller sample size.

Morphological investigations of AMPAR distributions after stimulation would also be interesting to do in the future. Our hypothesis states that rapid synaptic scaling should occur through internalization. If rapid synaptic scaling occurs it is still possible that AMPARs are not internalized, but rather that they diffuse laterally due to shrinking or dissolution of their nanostructures. Resolving AMPAR nanostructures requires super-resolution microscopy techniques due to their diffraction-limited size.

One way of approaching this would be to use stochastic optical reconstruction microscopy (STORM), with fluorescent antibodies for GluA1 and Bassoon to determine whether changes have occurred to synaptic AMPAR distribution [21]. Such an approach would see if synaptic scaling occurs through internalization – or through dynamic changes to AMPAR nanostructures. In fact, the original plan was to perform (or rather, optimize) a STORM protocol for the patched slices. It was for this reason that biocytin was routinely added to the pipette-solution. STORM was however not done, partly due to higher incidences of precautionary "sick-leave" of all interested parties (myself and supervisors), but also due to time constraints.

In conclusion, rapid synaptic scaling should be interrogated in a different experimental setup with a follow-up morphological investigation.

Populärvetenskaplig sammanfattning: Elektrofysiologiska undersökningar av synaptisk skalning i respons till optogenetiskt framkallade epilepsianfall

Din hjärna är en fantastisk apparat uppgjord av hundratals miljarder hjärnceller som var och en pratar med tiotusentals granneceller i ett makalöst nätverk-av-nätverk. För att förstå detta kan det vara hjälpsamt att likna hjärncellens form till ett träd – på detta *”träd”* är rötterna de så kallade dendriterna, och stammen som leder upp till kronan är den så kallade axonen. Celler bildar nätverk och pratar med varandra genom synapser, strukturer som delas mellan två celler: en *presynaptisk* cell vars axon möter dendriten hos en *postsynaptisk* cell. Hjärncellen använder dendriterna för att *”lyssna”* (ta emot signalinput) och axonen för att *”prata”* (skapa signaloutput) – *”trädet”* har alltså örat mot marken, men den talar rakt ut i luften.

Hjärnceller använder förstås inte ord eller ljud när de pratar, utan nervimpulssekvenser och signalsubstanser. Nervimpulser orsakar presynaptisk signalsubstansutsöndring mot receptorer på postsynapsen. Aktiverade receptorer orsakar jonflöde som påverkar cellmembranets elektriska spänning. Hur stor denna påverkan är beror på (1) utsöndringsgraden och (2) receptorantalet. Således är inputsignalens styrka reglerad på analogt vis. Om inputsignalen får membranspänningen att passera ett specifikt tröskelvärde kommer en nervimpuls skickas ner för axonen och därmed signalera andra celler. Denna tröskel gör outputsignalering till ett digitalt *”allt-eller-inget”* fenomen. Cellen kan därför tolkas som en analog-till-digital signalomvandlare – och på sätt och vis kan hela hjärnan därför jämföras med en dator.

Till skillnad från en dator så är hjärnans nätverk plastiska – formbara. Faktumet att du lärt dig läsa denna text är testamente till det. Att lära sig något är att forma hjärnan: när man exempelvis lär sig cykla så är de involverade cellerna ovana att aktiveras samtidigt, men med tid och repetition så blir dom bättre. Vad som egentligen händer är att nätverket som ansvarar för cykling förstärks genom att postsynapserna ökar antalet excitatoriska (aktivitetsfrämjande) receptorer, så att signalöverföringen blir mer effektiv. Inlärning är en form av så kallad Hebbiansk plasticitet, som ofta sammanfattas i frasen *”cells that fire together, wire together”*. Denna plasticitet är en positiv feedback-loop som ohejdat leder till aktivitetsexplosion. För att balansera detta krävs alltså någon form av negativ feedback, vilket hjärnan gör genom så kallad homeostatisk plasticitet. Synaptisk skalning är en homeostatisk mekanism, varuti antalet excitatoriska receptorer på *alla* synapser skalas enligt samma faktor, i motsats till Hebbiansk plasticitet som skalar receptorer på *enskilda* synapser. Synaptisk skalning tros ske inom loppet av timmar och dygn. Men för homeostatisk plasticitet att fungera måste den vara lika snabb som destabiliserande plasticiteters sammanläggning. Hur snabbt detta faktiskt är har inte utretts än. Det är därför intressant att se huruvida synaptisk skalning fungerar snabbare i epilepsi, en sjukdom präglad av nätverksinstabilitet. Epileptiska anfall är tillfällen av onormalt hög och samordnad nätverksaktivitet, och är oftast bara några minuter långa. Om synaptisk skalning reagerar på epileptiska anfall skulle det antyda att skalning sker mycket snabbare än man tror.

För att undersöka detta gjordes en epileptisk anfallsmodell i mushippocampus med hjälp av *optogenetik*, en teknik varuti man gör celler ljuskänsliga. Snabbt blinkande ljus kan då orsaka onormalt hög och samordnad nätverksaktivitet – alltså en kontrollerbar epilepsianfallsmodell. Genom att mäta cellers elektriska profiler ville vi se om deras basaktivitet sänks i respons till optogenetiska epilepsianfall. Detta ska nämligen ske om alla synapser blir försvagade enligt synaptisk skalning. Mätningarna gjordes genom *whole-cell patch-clamping*, en elektrofysiologisk teknik varuti man *”punkterar”* en cell med en glaspipettbeträdd elektrod för att mäta dess elektriska profil. Våra resultat kunde dessvärre varken påvisa eller utesluta existensen av en *”snabb”* form av synaptisk skalning. Med små modifikationer till det experimentella upplägget kommer framtida forskning förhoppningsvis kunna svara på denna intressanta fråga.

Acknowledgements

First, I would like to thank Professor Merab Kokaia for inviting me into the Experimental Epilepsy Group. Your trust in me and my abilities has meant a great deal to me. Secondly, I would like to thank Professor Leif Bülow, for agreeing to be my examiner and for always encouraging me to do the best that I can do. I would also like to extend my thanks to Marco Ledri, for teaching me how to patch clamp, but more importantly for showing me that rock-star and scientist are not mutually exclusive professions; to My Andersson, for talks on chili, the moon-lander, tabletop games, podcasts – and everything in between; to Jan Kudláček, for dancing to Vulfpeck and proving that friends can be made despite a raging pandemic; to Apostolos Mikroulis, for helping with data analysis, and more importantly for teaching me the importance of *darkness*; to Eliška Waloschková for having fun, fun, fun with the kazoo; to Ana Gonzalez Ramos, for the warmth and happiness that you spread; to Ling Cao and Susanne Geres, for genotyping mice and helping me whenever disaster struck; to Fredrik Berglind, for talks on life on the bus; to Esbjörn Melin, for the beer and science-talks; to my mom, my dad, and my brothers – for everything. Finally, I would like to thank the love of my life, Sanna. You make me a better person.

References

1. Kandel ERS, James H.; Jessell, Thomas M.; Siegelbaum, Steven A.; Hudspeth, A. J. Principles of Neural Science. Fifth ed: The McGraw-Hill Companies Inc. ; 2013. 1760 p.
2. Berg AT, Berkovic SF, Brodie MJ, Buchhalter J, Cross JH, Van Emde Boas W, et al. Revised terminology and concepts for organization of seizures and epilepsies: Report of the ILAE Commission on Classification and Terminology, 2005-2009. Epilepsia. 2010;51(4):676-85.
3. Updyke M, Duryea B. To Provoke or Not Provoke: Ethical Considerations in the Epilepsy Monitoring Unit. Journal of Neuroscience Nursing. 2013;45(3).
4. Jenssen S, Gracely EJ, Sperling MR. How Long Do Most Seizures Last? A Systematic Comparison of Seizures Recorded in the Epilepsy Monitoring Unit. Epilepsia. 2006;47(9):1499-503.
5. Zubler F, Steimer A, Gast H, Schindler KA. Seizure Termination. Elsevier; 2014. p. 187-207.
6. Lignani G, Baldelli P, Marra V. Homeostatic Plasticity in Epilepsy. Frontiers in Cellular Neuroscience. 2020;14(197).
7. Turrigiano GG, Nelson SB. Homeostatic plasticity in the developing nervous system. Nature Reviews Neuroscience. 2004;5(2):97-107.
8. Rogawski MA. AMPA receptors as a molecular target in epilepsy therapy. Acta Neurologica Scandinavica. 2013;127:9-18.
9. Wu YK, Hengen KB, Turrigiano GG, Gjorgjieva J. Homeostatic mechanisms regulate distinct aspects of cortical circuit dynamics. Proceedings of the National Academy of Sciences. 2020;117(39):24514.
10. Masland RH. Neuronal cell types. Current Biology. 2004;14(13):R497-R500.
11. Wu Y, Chen H, Guo L. Opportunities and dilemmas of in vitro nano neural electrodes. RSC Advances. 2020;10(1):187-200.
12. Raichle ME, Gusnard DA. Appraising the brain's energy budget. Proceedings of the National Academy of Sciences. 2002;99(16):10237-9.
13. Hodgkin AL, Huxley AF. A quantitative description of membrane current and its application to conduction and excitation in nerve. The Journal of Physiology. 1952;117(4):500-44.
14. Devices M. What is an action potential? : Molecular Devices; [Available from: https://www.moleculardevices.com/applications/patch-clamp-electrophysiology/what-action-potential.
15. Århem P, Klement G, Blomberg C. Channel Density Regulation of Firing Patterns in a Cortical Neuron Model. Biophysical Journal. 2006;90(12):4392-404.
16. Qu L, Akbergenova Y, Hu Y, Schikorski T. Synapse-to-synapse variation in mean synaptic vesicle size and its relationship with synaptic morphology and function. The Journal of Comparative Neurology. 2009;514(4):343-52.
17. Park M. AMPA Receptor Trafficking for Postsynaptic Potentiation. Frontiers in Cellular Neuroscience. 2018;12.
18. Park P, Kang H, Sanderson TM, Bortolotto ZA, Georgiou J, Zhuo M, et al. The Role of Calcium-Permeable AMPARs in Long-Term Potentiation at Principal Neurons in the Rodent Hippocampus. Frontiers in Synaptic Neuroscience. 2018;10.
19. Mayer ML. Glutamate receptor ion channels. Current Opinion in Neurobiology. 2005;15(3):282-8.

20. Armstrong N, Jasti J, Beich-Frandsen M, Gouaux E. Measurement of Conformational Changes accompanying Desensitization in an Ionotropic Glutamate Receptor. Cell. 2006;127(1):85-97.
21. Nair D, Hosy E, Petersen JD, Constals A, Giannone G, Choquet D, et al. Super-resolution imaging reveals that AMPA receptors inside synapses are dynamically organized in nanodomains regulated by PSD95. J Neurosci. 2013;33(32):13204-24.
22. College O. Communication Between Neurons. 2021. In: Anatomy & Physiology [Internet]. www.lumenlearning.com: Rice University. Available from: https://courses.lumenlearning.com/suny-ap1/chapter/communication-between-neurons/.
23. Malkin SL, Kim KK, Tikhonov DB, Zaitsev AV. Properties of spontaneous and miniature excitatory postsynaptic currents in neurons of the rat prefrontal cortex. Journal of Evolutionary Biochemistry and Physiology. 2014;50(6):506-14.
24. Murthy VN. Synaptic plasticity: Step-wise strengthening. Current Biology. 1998;8(18):R650-R3.
25. The Nobel Prize in Physiology or Medicine 1991 [press release]. NobelPrize.org, 2021-01-03 2021.
26. Grant G. The Nobel Prizes in the field of neuroscience-from Camillo Golgi and Ramón y Cajal to John 0'Keefe and May-Britt Moser and Edvard I Moser nobelprizemedicine.org [Available from: https://www.nobelprizemedicine.org/selecting-laureates/history/the-nobel-prizes-in-the-field-of-neuroscience/.
27. Ypey DL, DeFelice L, editors. The patch-clamp technique explained and exercised with the use of simple electrical equivalent circuits2007.
28. Suchyna TM, Markin VS, Sachs F. Biophysics and Structure of the Patch and the Gigaseal. Biophysical Journal. 2009;97(3):738-47.
29. Carter M, Shieh J. Electrophysiology. Elsevier; 2015. p. 89-115.
30. Devices M. Electrophysiology: Molecular Devices; 2021 [Available from: https://www.moleculardevices.com/technology/electrophysiology.
31. Neher E, Sakmann B. The Patch Clamp Technique. Scientific American. 1992;266(3):44-51.
32. Veitinger SPUM, Institute of Cytobiology and Cytopathology. The Patch-Clamp Technique An Introduction: Leica Microsystems; 2011 [Available from: https://www.leica-microsystems.com/science-lab/the-patch-clamp-technique/.
33. Tung JK, Berglund K, Gross RE. Optogenetic Approaches for Controlling Seizure Activity. Brain Stimulation. 2016;9(6):801-10.
34. Pastrana E. Optogenetics: controlling cell function with light. Nature Methods. 2011;8(1):24-5.
35. Zemelman BV, Lee GA, Ng M, Miesenböck G. Selective Photostimulation of Genetically ChARGed Neurons. Neuron. 2002;33(1):15-22.
36. Boyden ES, Zhang F, Bamberg E, Nagel G, Deisseroth K. Millisecond-timescale, genetically targeted optical control of neural activity. Nature Neuroscience. 2005;8(9):1263-8.
37. Gradinaru V, Thompson KR, Deisseroth K. eNpHR: a Natronomonas halorhodopsin enhanced for optogenetic applications. Brain Cell Biology. 2008;36(1-4):129-39.
38. Araki K, Araki M, Yamamura KI. Targeted integration of DNA using mutant lox sites in embryonic stem cells. 1997;25(4):868-72.
39. Erondu N, Kennedy M. Regional distribution of type II Ca2+/calmodulin-dependent protein kinase in rat brain. The Journal of Neuroscience. 1985;5(12):3270-7.
40. Au - Van Hoeymissen E, Au - Philippaert K, Au - Vennekens R, Au - Vriens J, Au - Held K. Horizontal Hippocampal Slices of the Mouse Brain. JoVE. 2020(163):e61753.

41. Duvernoy HM. The Human Hippocampus: Functional Anatomy, Vascularization and Serial Sections with MRI. 3 ed: Springer Berlin Heidelberg; 2005. 232 p.
42. Milior G, Di Castro MA, Sciarria LP, Garofalo S, Branchi I, Ragozzino D, et al. Electrophysiological Properties of CA1 Pyramidal Neurons along the Longitudinal Axis of the Mouse Hippocampus. Scientific Reports. 2016;6(1):38242.
43. Malenka RC, Bear MF. LTP and LTD. Neuron. 2004;44(1):5-21.
44. Fuchs E, Flügge G. Adult Neuroplasticity: More Than 40 Years of Research. Neural Plasticity. 2014;2014:1-10.
45. Leuner B, Gould E. Structural Plasticity and Hippocampal Function. Annual Review of Psychology. 2010;61(1):111-40.
46. Miller KD. Synaptic Economics: Competition and Cooperation in Synaptic Plasticity. Neuron. 1996;17(3):371-4.
47. Bear MF, Malenka RC. Synaptic plasticity: LTP and LTD. Curr Opin Neurobiol. 1994;4(3):389-99.
48. Katz LC, Crowley JC. Development of cortical circuits: Lessons from ocular dominance columns. Nature Reviews Neuroscience. 2002;3(1):34-42.
49. Turrigiano GG, Leslie KR, Desai NS, Rutherford LC, Nelson SB. Activity-dependent scaling of quantal amplitude in neocortical neurons. Nature. 1998;391(6670):892-6.
50. Turrigiano GG. The self-tuning neuron: synaptic scaling of excitatory synapses. Cell. 2008;135(3):422-35.
51. Turrigiano G. Homeostatic synaptic plasticity: local and global mechanisms for stabilizing neuronal function. Cold Spring Harbor perspectives in biology. 2012;4 1:a005736.
52. Shneker BF, Fountain NB. Epilepsy. Disease-a-Month. 2003;49(7):426-78.
53. Pitkänen A, Lukasiuk K, Dudek FE, Staley KJ. Epileptogenesis. Cold Spring Harb Perspect Med. 2015;5(10):a022822.
54. Stafstrom CE, Carmant L. Seizures and epilepsy: an overview for neuroscientists. Cold Spring Harb Perspect Med. 2015;5(6):a022426.
55. Rukhsar S, Rehman H, Khan YU, Khan AT, editors. Detection of epileptic seizure in EEG signals using phase space reconstruction and euclidean distance of first-order derivative2017: IEEE.
56. Huynh TD, Ashraf O, Craig H, Larmeu L, Barker B, Stephenson C, et al. Optogenetic activation of CA1 pyramidal neurons in vivo induces hypersynchronous and low voltage fast seizures. 2020.
57. Choi S, Lovinger DM. Decreased Frequency But Not Amplitude of Quantal Synaptic Responses Associated with Expression of Corticostriatal Long-Term Depression. The Journal of Neuroscience. 1997;17(21):8613-20.
58. Grubb MS, Burrone J. Channelrhodopsin-2 Localised to the Axon Initial Segment. PLoS ONE. 2010;5(10):e13761.
59. Rodriguez G, Mesik L, Gao M, Parkins S, Saha R, Lee H-K. Disruption of NMDAR Function Prevents Normal Experience-Dependent Homeostatic Synaptic Plasticity in Mouse Primary Visual Cortex. The Journal of Neuroscience. 2019;39(39):7664-73.
60. Reimers JM, Milovanovic M, Wolf ME. Quantitative analysis of AMPA receptor subunit composition in addiction-related brain regions. Brain Res. 2011;1367:223-33.
61. Goold CP, Nicoll RA. Single-Cell Optogenetic Excitation Drives Homeostatic Synaptic Depression. 2010;68(3):512-28.
62. Williams SR, Mitchell SJ. Direct measurement of somatic voltage clamp errors in central neurons. Nature Neuroscience. 2008;11(7):790-8.

63. Bar-Yehuda D, Korngreen A. Space-clamp problems when voltage clamping neurons expressing voltage-gated conductances. J Neurophysiol. 2008;99(3):1127-36.
64. Olsen RW. Picrotoxin-like channel blockers of GABAA receptors. Proc Natl Acad Sci U S A. 2006;103(16):6081-2.
65. Vierock J, Rodriguez-Rozada S, Pieper F, Dieter A, Bergs A, Zeitzschel N, et al. BiPOLES: a tool for bidirectional dual-color optogenetic control of neurons. 2020.